Fall 1-27-2008

Multi well uni-axial stretch injury device

Mridusmita Choudhury
New Jersey Institute of Technology

Copyright Warning & Restrictions

The copyright law of the United States (Title 17, United States Code) governs the making of photocopies or other reproductions of copyrighted material.

Under certain conditions specified in the law, libraries and archives are authorized to furnish a photocopy or other reproduction. One of these specified conditions is that the photocopy or reproduction is not to be "used for any purpose other than private study, scholarship, or research." If a, user makes a request for, or later uses, a photocopy or reproduction for purposes in excess of "fair use" that user may be liable for copyright infringement,

This institution reserves the right to refuse to accept a copying order if, in its judgment, fulfillment of the order would involve violation of copyright law.

Please Note: The author retains the copyright while the New Jersey Institute of Technology reserves the right to distribute this thesis or dissertation

Printing note: If you do not wish to print this page, then select "Pages from: first page # to: last page #" on the print dialog screen

ABSTRACT

MULTI WELL UNI-AXIAL STRETCH INJURY DEVICE

by
Mridusmita Choudhury

Most diffuse brain injury is the result of uni-axial stretch of brain axons in traumatic brain injury. Traumatic injury to axons throughout the brain and is believed to be a major cause for coma, and other complications. Diffuse axonal injury is mostly multi-focal and appears throughout the deep cortical and sub-cortical regions.

Several models have tried to replicate this phenomenon. Previous models, like the Penn model, have lower throughput as they conduct experiments on one well at a time, and it has lower reproducibility as well. The other problem with these models is that they are not very user friendly, and extensive experience is required to get some consistence in the results.

The goal of this project is to create a high throughput, cost effective, and user friendly, in-vitro model for uni-axial stretch of axons to simulate the effect of TBI on the neurons of the brain. My endeavor is to create an in-vitro model for uni-axial stretch of axons to namely a "Multi-Well Axonal Stretch Injury Device" to induce strains or stretch rates in the magnitude of 10% to 80% on axons to simulate mild to moderate to severe traumatic brain injury. The cells used for primary experimentation will be the NG-108 cell lines. This project will include the design, development and testing procedure for this device. Both mechanical characterization and biological viability studies will be conducted to test the device.

MULTI WELL UNI-AXIAL STRETCH INJURY DEVICE

by
Mridusmita Choudhury

A Thesis
Submitted to the Faculty of
New Jersey Institute of Technology
in Partial Fulfillment of the Requirements for the Degree of
Master of Science in Biomedical Engineering

Department of Biomedical Engineering

January 2008

APPROVAL PAGE

MULTI WELL UNI-AXIAL STRETCH INJURY DEVICE

Mridusmita Choudhury

Dr. Bryan J. Pfister, Thesis Advisor Assistant Professor of Biomedical Engineering, NJIT	Date
Dr. Richard Foulds, Committee Member Professor of Biomedical Engineering, NJIT	Date
Dr. Max Roman, Committee Member Professor of Biomedical Engineering, NJIT	Date
Lisa Schmidt, Committee Member Director of Engineering, Herbst Research, Inc	Date

BIOGRAPHICAL SKETCH

Author: Mridusmita Choudhury

Degree: Master of Science

Date: January 2008

Undergraduate and Graduate Education:

- Master of Science in Biomedical Engineering,
  New Jersey Institute of Technology, Newark, NJ, 2008

- Bachelor of Engineering in Electronic Engineering,
  D J Sanghvi College Of Engineering, Mumbai University, India, 2005

Major: Biomedical Engineering

To my beloved family

ACKNOWLEDGMENT

I would like to express my deepest appreciation to Dr. Bryan Pfister, who not only served as my research supervisor, providing valuable and countless resources, insight, and intuition, but also constantly gave me support, encouragement, and reassurance. Without his help, I would not have completed this thesis.

Special thanks are given to Dr. Richard Foulds, Dr. Max Roman and Lisa Schmidt for actively participating in my committee. I would especially like to thank Lisa Schmidt for providing me valuable information, and troubleshooting suggestions.

I would also like to thank my colleagues at Dr. Pfister's laboratory and all my friends for their constant feedback and support.

Finally I would like to express my deepest gratitude to my parents, and my sisters for their unfailing support, immeasurable sacrifices, and their belief in me.

TABLE OF CONTENTS

TABLE OF CONTENTS
(Continued)

Chapter **Page**

LIST OF FIGURES

LIST OF FIGURES
(Continued)

CHAPTER 1

INTRODUCTION

1.1 Objective

Traumatic brain injury is a leading cause of death and disability in the world. The incidence of TBI is higher than spinal cord injury, muscular dystrophy, multiple sclerosis, and a host of other neurological disorders, with one person getting affected every 15 seconds or less [1]. Statistics show that traumatic brain injury is most likely to cause permanent physical, emotional, and mental disability than much other neurological pathology. [2, 3, 4, 5, 6, 7].

Traumatic brain injury is characterized by mechanical deformations in the brain resulting in microscopic and macroscopic "stretch" of brain tissue and in particular axons [1, 9, 10, 11, 12, 13]. The effect of uniaxial stretch on axons is a challenge to study in vivo due to its microscopic nature. For example, histopathological studies must be performed post-mortem and offers little information about the progression of the injury. To overcome this disadvantage and monitor the real-time effects of axonal stretch injury an efficient, accurate, and high yield *in vitro* model is required.

In this project, the author's endeavor is to develop an *in vitro* model to induce uniaxial stretch injury to cultured axons within a "Multi-Well Axonal Stretch Injury Device". This device will induce strains of 10% to 80% on axons to simulate mild, moderate or severe traumatic brain injury [14]. The cells used for primary experimentation will be the NG-108 cell lines. This project will include the design,

development and testing procedure for this device. Both mechanical characterization and biological viability studies will be conducted to test the device.

1.2 Background Information

Statistics show that in the United States alone 1.4 million people suffer from Traumatic Brain Injury out of which 50,000 die, and 1.1 million people are admitted in medical emergency cases. Among children in the age group of 0 to 14 years, there were 2685 deaths and 37,000 hospitalizations [8].

Traumatic brain injury can be of two types, localized or "focal" brain injury which results from blows to the head and may result in hemotomas and contusions. Secondly it could be widespread or "diffuse" which occurs in the absence of impact and is due to inertial forces due to rotational motion induced in motor accidents for both the driver and the pedestrian or assaults [12]. The unpredictable component in traumatic brain injury is that many symptoms may occur hours or even days after the injury.

1.2.1 Symptoms and Axonal Effects

The extent of brain injury can vary from mild to moderate to severe. Symptoms of mild TBI include loss of consciousness for a few seconds or minutes, headache, confusion, lightheadedness, dizziness, blurred vision or tired eyes, ringing in the ears, bad taste in the mouth, fatigue or lethargy, a change in sleep patterns, behavioral or mood changes, and trouble with memory, concentration, attention, or thinking. Moderate or severe TBI symptoms may include nausea, convulsions or seizures, an inability to awaken from sleep, dilation of one or both pupils of the eyes, slurred speech, weakness or numbness in the extremities, loss of coordination, and increased confusion, restlessness, or

agitation [8].

At the microscopic level, mild and moderate TBI result in swollen and disconnected axons. At the macroscopic level the brain tissue appears to be unharmed and hence is undetected in radiological screening [12]. In severe cases of TBI macroscopic tears in brain tissue is observed and the extensive diffuse axonal injury is associated with poor patient outcome including mortality rate, and coma [12].

1.2.2 Mechanical Forces Causing Uni-axial Stretch Of Axons

Mechanical deformation of brain tissue is the primary event in any traumatic brain injury. As in the case of most head injuries, rapid rotational motion of the head leads to shear deformation of the brain tissue due to inertial forces acting on it. This is shown by biomechanical studies involving a silicone filled pig's skull [12, 16] as silicone has similar viscoelastic properties as brain tissue. Imaging techniques from this experiment provides evidence that in shear deformation of the brain tissue in rotational head injuries translates microscopically to rapid longitudinal or uni-axial stretching of axons fibers along the diagonal of the shear forces [12]. Figure 1.1 is a representation of uni-axial stretch in a shear deformation. The dotted line shows the path of uni-axial stretch in the block of matter, or the brain.

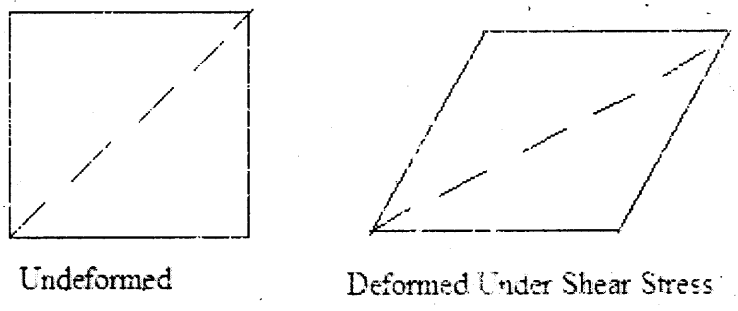

Figure 1.1 Representation of uni-axial or longitudinal stretch in shear deformation.

Uni-axial stretch can be induced on the membrane is several ways. Other *in vitro* and *in vivo* models use air pressure pulse to induce uni-axial stretch on axons. Studies have shown that pressure deformation curves are linear for silicone membrane and silastic membranes [15]. Since the pressure-deformation relationship is linear, the deformation of the silicone membrane and attached axons follows the pressure curve. For example, for a particular pressure applied to a silicone well a particular stretch is achieved which in turn translates into a particular strain on the axons cultured in that well.

The important parameters in controlling and monitoring the membrane deformation are the rise time of the pressure pulse, which represents the rate of stretch (speed of injury) or strain rate and the peak pressure, which represents the peak deformation of the membrane and attached axons. A typical pressure pulse recorded by the Penn device is shown in Figure 1.2.

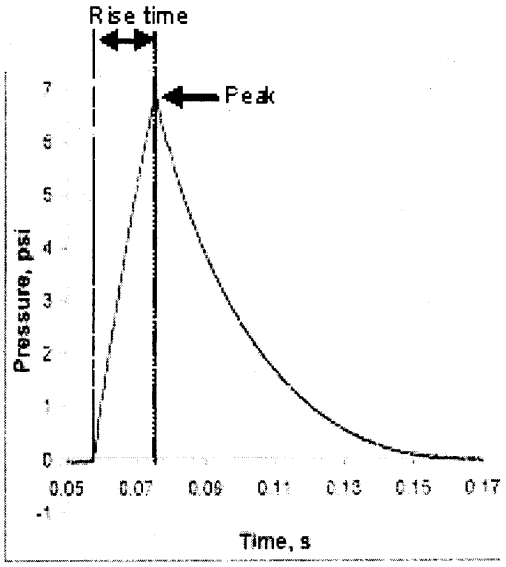

Figure 1.2 Pressure pulse from Penn Device recorded by Dr. Bryan Pfister.

The pressurization of the injury pressure chamber is affected by both the input pressure and the time the solenoid valve is open or the response time of the valve. The input pressure is the driving force affecting the rate of pressure increase and peak pressure, and the opening and closing of the solenoid valve places a limit on the rise time. These two parameters can be adjusted independently to achieve various strains and strain rates. Previous *in vitro* models have lower control over these parameters due to limited design and component capability

1.2.3 Previous *In vitro* Models

Previous *in vitro* models include the injury device models in Virginia Commonwealth University called 94A Cell Injury Controller, and University of Pennsylvania here referred to as the "Penn model" [15]. In the 94A Cell Injury Controller the inlet is connected to a tank of compressed gas, and a valve and timer are used to control the time and duration of the pressure pulse. There are six wells in this device and a separate pressure pulse is required for each well. The membrane deformation is measured by three ways including a sliding pointer method, a video-camera method, and by making molds using dental acrylate. From the membrane deformation strains and strain rates were duly calculated.

The Penn model is unique in its isolation of axons for uni-axial stretch injury. However, this model again deflects one well at a time. This procedure is limited by low yield, sample to sample variation, bad control of the pressure pulse subjected to the membrane, and low biocompatibility. The reason for this variability is that only a regulator is used to connect the main air tank supply to the solenoid valve. Due to limited

capability of the regulator with respect to the maximum air flow, a constant driving pressure force cannot be maintained and variable pressure pulses are obtained. Figure 1.3 shows the air flow diagram of the Penn model.

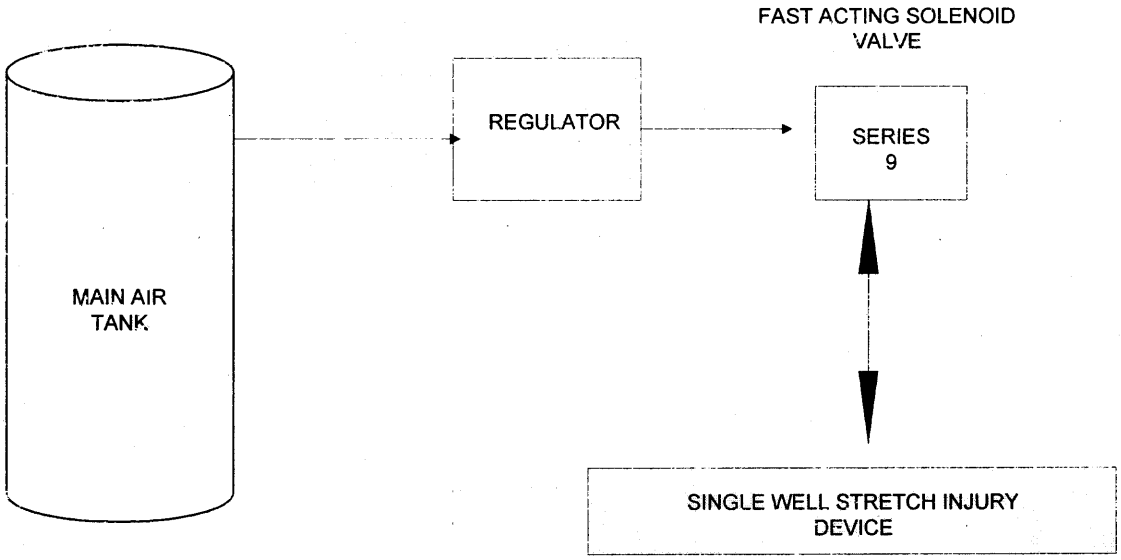

Figure 1.3 Air Flow diagram of Penn Model.

The other disadvantage of the Penn model is that the stainless steel wells were found to be toxic to cells. In the author's design, PEEK (polyetheretherketone) plastic is used to replace the stainless steel wells to lower toxicity to cells.

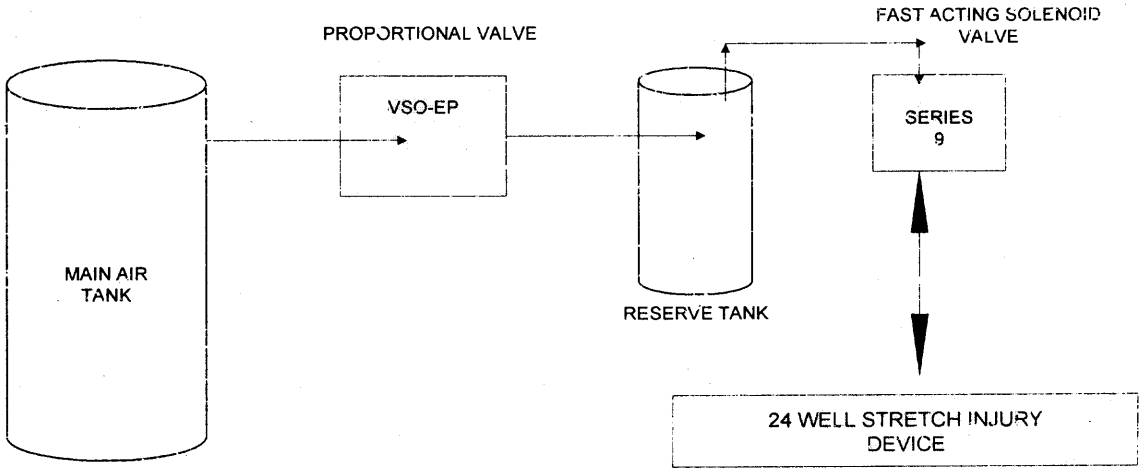

Figure 1.4 Air flow diagram for Multi Well Injury Device.

A comparison of the air flow diagrams of the Penn model in Figure 1.3 and the author's model in Figure 1.4 shows that the Penn model is more simplified and does not have a reserve volume. As the regulator has a limitation on maximum air flow, the driving pressure from the regulator is not constant and results in a variable (decreasing) driving force during delivery of the pressure pulse. Hence, inconsistent results are often obtained from the Penn model for repeated attempts. Another drawback in the Penn model design is that the solenoid valve used has an optimal opening response (15-20 ms) and is limited to an input pressure of 50 psi. Due to this short rise times cannot be accurately realized in the Penn model. The slope of the pressure pulse denotes strain rate, and if short rise time cannot be maintained high strain rates cannot be achieved. To achieve higher strain rates as described in the previous section, a higher driving pressure force is required as well as a faster response time for the solenoid valve. The Series 9valve selected in the author's design addresses both these problems as described in the Materials and Methods section.

CHAPTER 2

MATERIALS AND METHODS

2.1 System Introduction

In this project, the author's endeavor is to create a high throughput, cost effective, and user friendly, *in vitro* model for uniaxial stretch of axons to simulate the effect of TBI on the axons of the brain. The objective of the control system is to produce a reproducible pressure pulse like the one in the Penn model as shown in Figure 1.2. For this "Multi-Well Axonal Stretch Injury Device" the design parameters call for an air pulse of about 7 psi within a 20 ms period. This pulse, used for the Penn device, delivers 60% strain at a strain rate of 20 s^{-1}. To increase sample throughput, a 24 well PEEK plate is designed similar to a standard 24 well tissue culture plate, with a deformable silicone membrane stretched across its base for cell culture to deliver stretch injury. This plate is placed in a pressure chamber where the precise pressure pulse is delivered via an automated control system based in Labview 7.1 (National Instruments).

The "Multi Well Axonal Stretch Injury Device'' has both a control and an injury device sub-system. An overview of the system has been shown in Figure 2.1.The two subsystems, namely the control subsystem and the injury device subsystem with the list of components have been discussed hereafter.

2.2 Control Subsystem

The electrical subsystem is used for controlling the injury device subsystem. This system consists of the electro-mechanical valves, DAQ card (NI-6009) for the computer

interface, and the computer. Several valves used to control this device. A comparison of the air flow of the previous *in vitro* model the Penn device and the author's design has been shown in Figures 2.1 and 2.2.

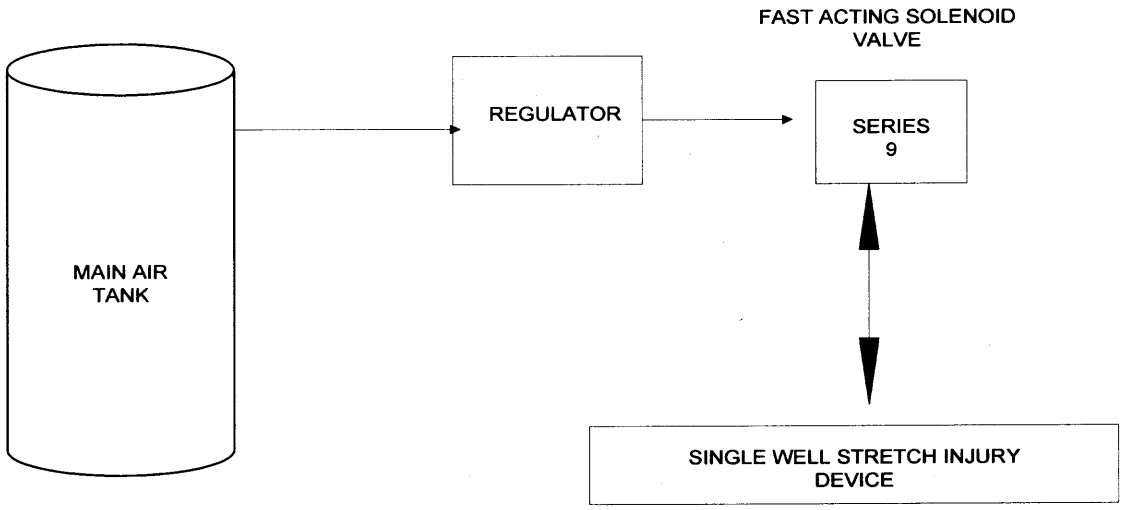

Figure 2.1 Air Flow in Penn Model.

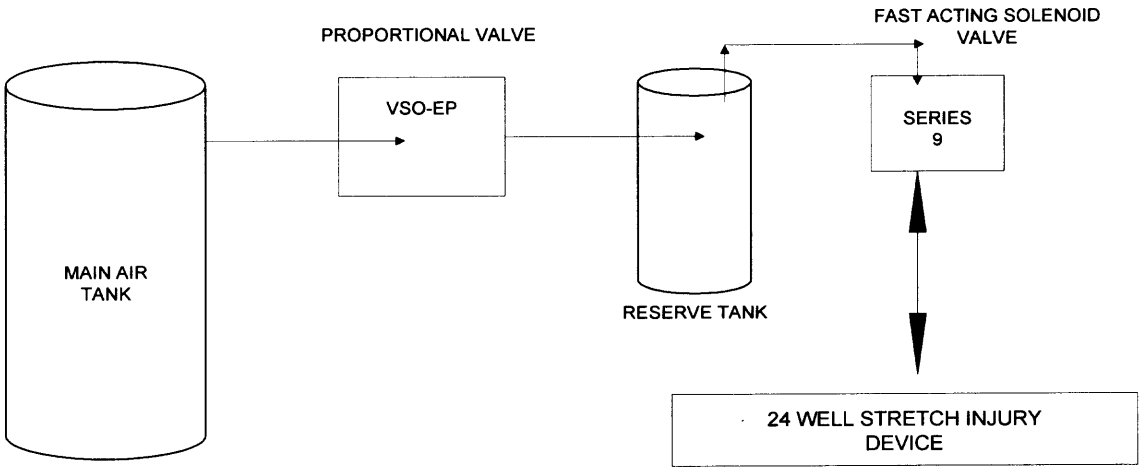

Figure 2.2 Air flow in author's model.

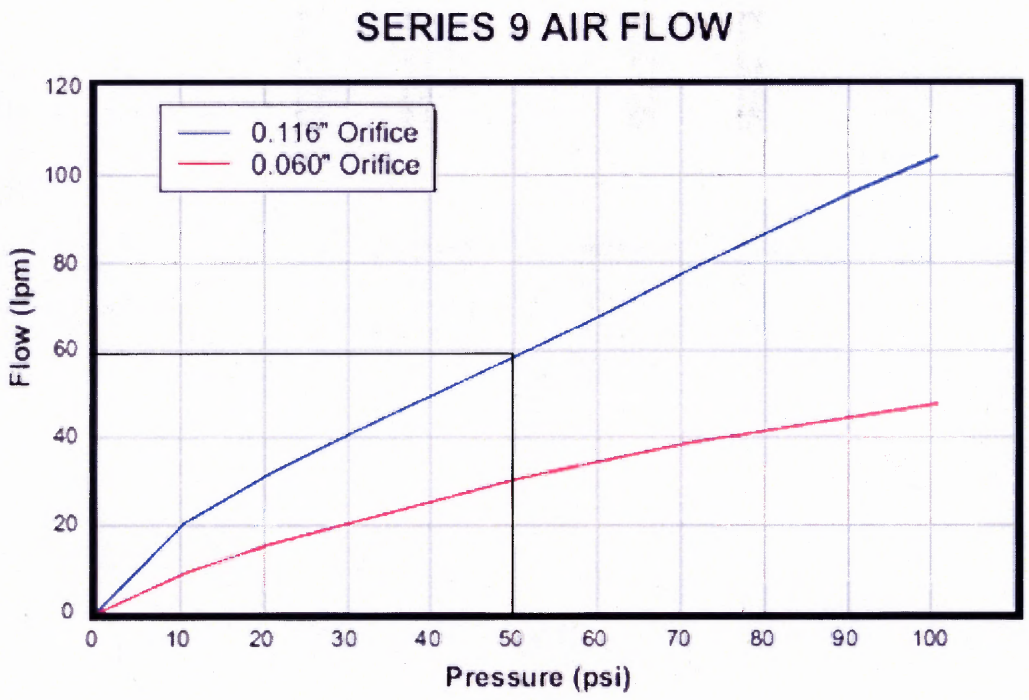

Figure 2.3 Flow characteristics of fast acting solenoid valve (Series 9).

The flow characteristics of the fast acting solenoid valve (Series 9 valve) are shown in Figure 2.3. The orifice size used by the author in this study is the 0.116 inch solenoid valve. From this curve, at an operating pressure of 50 psi, the flow rate of air is about 60 lpm (litres per minute). Hence for faster response time, the driving pressure must be higher to overcome the frictional forces in the tubing.

To understand the flow characteristics in each inlet of the 4-way manifold the Reynold's number is calculated for each inlet. Assuming a lossless system, the flow rate (Q) in each tube can be given by

$$Q = VA$$

where V is the velocity of fluid in the tube and A is the area of the tube. The flow rate through each of the 4 tubes is 15 lpm. Therefore, the velocity through each tube is 15.44 m/s.

The Reynold's number identifies the type of flow as laminar, turbulent, or transitional. It can be calculated using the following equation.

$$Re = VD/ (\upsilon/\rho)$$

where V is the velocity of the fluid, D is the diameter of the tube, υ is the viscosity of air, and ρ is the density of air. At 20 °C (room temperature), the viscosity of air is 1.8×10^{-5} kg/m-s, and its density is 1.2 kg/ m^3.

$$Re = \frac{(15.44 \text{ m/s})\ (4.54 \times 10^{-3} \text{ m})}{(1.8 \times 10^{-5} \text{ kg/m-s})/\ 1.2 \text{ kg/ m}^3}$$

$$Re = 4673$$

Therefore, the flow through each tube is just turning turbulent.

The control system as shown in figure 2.3 controls the air flow of the injury device. The individual components of the control system will be discussed hereafter.

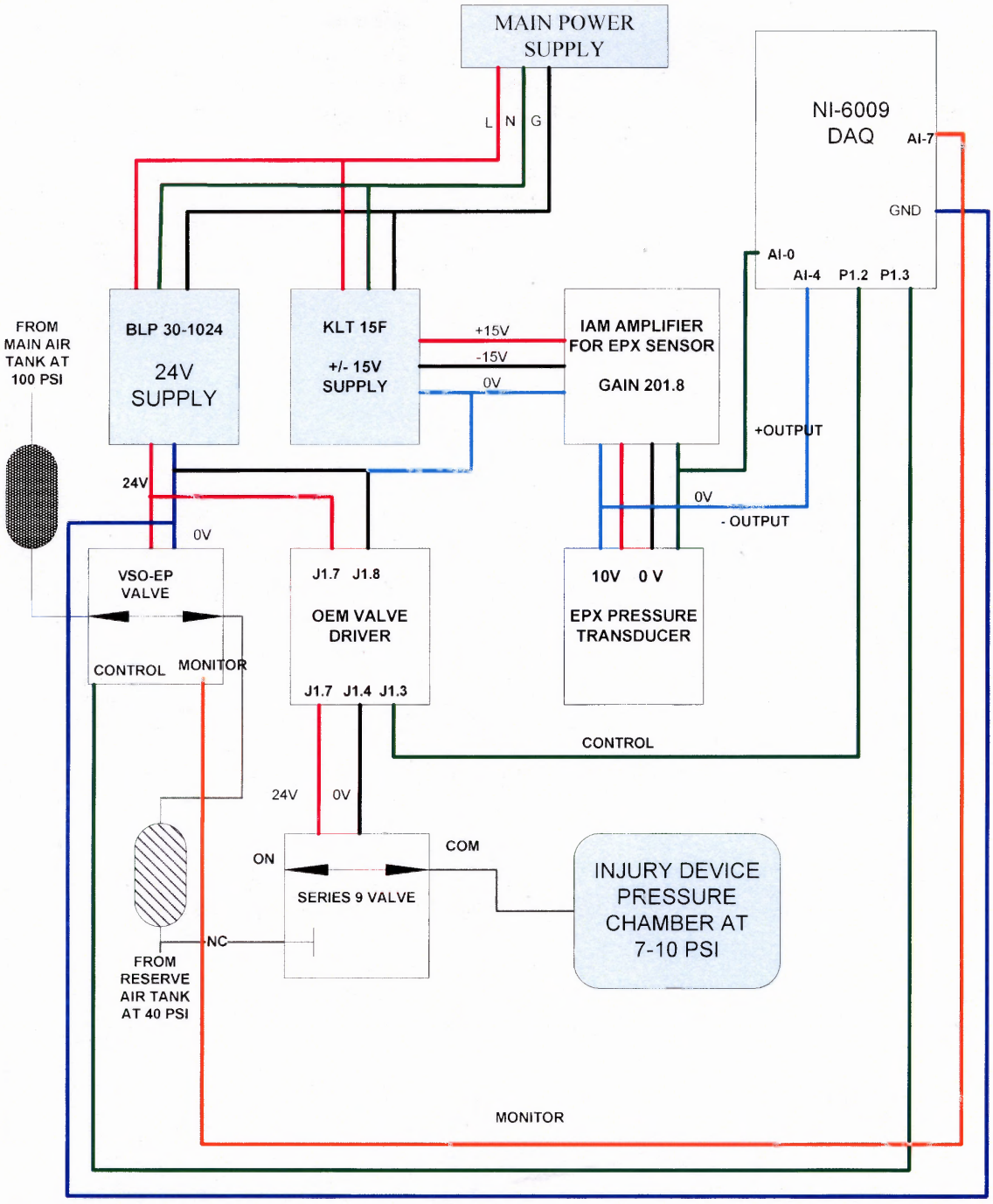

Figure 2.4 Control system overview.

2.2.1 VSO-EP Electronic Pressure Control Unit

A proportional valve is used to control the air flow from the main air tank into the reserve air tank. It has a close loop system which maintains a set pressure from 0 to 100 psi using a pressure transducer. The proportional valve used here is the VSO-EP Electronic Pressure Control Unit from Parker Hannifin Corporation. This unit converts a variable electrical control signal into a variable pneumatic output.

The key feature in the author's decision was the response time of the valve, which is 15 ms and is one of the fastest available proportional valves in the market. The other desirable features of this valve were the size, the power capability, and the longevity of the product. This valve is controlled by the control input line of the valve which is hooked up to the NI-6009 DAQ card. Once the control input line is set to a certain user defined voltage, the valve switches on and allows the main air cylinder to pressurize the reserve tank to a pressure directly proportional to the voltage supplied. The internal pressure transducer of the VSO-EP Electronic Pressure Control Unit allows the monitoring of the pressure at the reserve tank end via Labview7.1 interface. Proportional valves work on the principle of opening in "proportion" to supply voltage. Hence proportional valves are very useful for maintaining pressure levels. This feature allows the author to use the VSO-EP valve for testing the apparatus and characterizing the injury device as described in the "Testing and Device Characterization" section.

2.2.2 Series 9 Extreme Performance Valve

Once the reserve tank is pressurized to a desired pressure, a control signal is set to drive a three-way normally closed fast acting solenoid valve to pressurize the injury device pressure chamber. Our goal is to pressurize the chamber to 7-10 psi within 20 ms, and de-

pressurize it within the next 100 ms. The solenoid fast acting valve used by the author is the Series 9 valve by Parker Hannifin Corporation. The three-way valve depressurizes the chamber by venting upon closure. The key feature in the author's decision was the response time of the valve, which is less than 5 ms and is the fastest available solenoid valve the author could identify in the market. The other desirable features of this valve were the size, the power capability, and the longevity of the product.

2.2.3 OEM Valve Driver

The Series 9 valve is driven by OEM Valve Driver whose control input line of is hooked up to the NI-6009 DAQ card. Once the control input line is set to high, the driver switches on to open the Series 9 solenoid valve and allows the reserve air tank to pressurize the main air chamber to a user set pressure. When control input is high, the OEM Valve Driver provides an excitation of 10 V to the Series 9 Valve for the user specified amount of time. In this case, the Series 9 Valve is required to be on till the pressure within the air chamber reaches 7 psi, and it switches off to depressurize the injury device pressure chamber to 0 psi. The OEM valve driver hence controls the opening and closing time of the solenoid valve (Series 9 Extreme Performance Valve).

For future applications, the OEM valve driver can also be used to overdrive the solenoid valve to further reduce opening time of the Series 9 valve. This can be achieved by applying a high voltage for a period of time before pulling down the applied voltage to a recommended level. Figure 2.4 is a hypothetical pulse applied to overdrive the solenoid valve via the OEM valve driver.

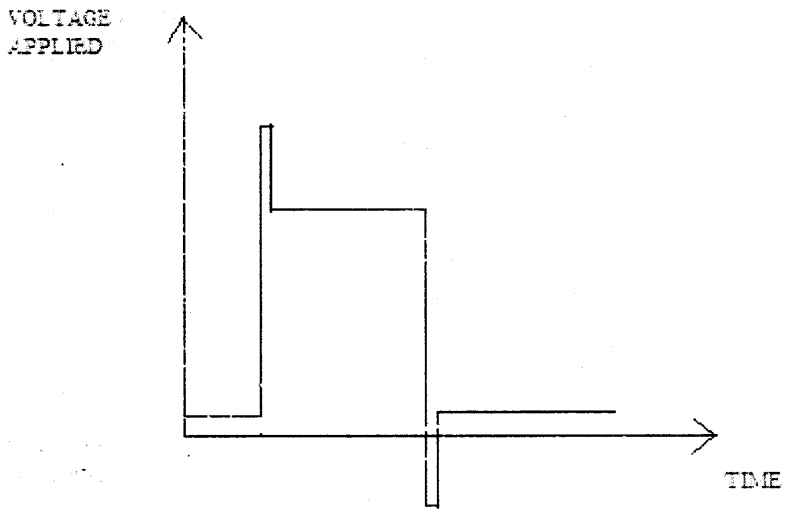

Figure 2.5 Hypothetical voltage pulse used to overdrive and under-drive solenoid valve.

2.2.4 Safety Pop Valves

Safety pop valves of 100 psi and 150 psi are also used to prevent the air tanks from reaching pressures higher than the maximum allowed input pressures into the valves and thereby protecting the valves. The main air cylinder is at 150 psi limit and the reserve tank is at 100 psi limit so that it allows a forward air flow by having the driving pressure higher than the reserve tank pressure.

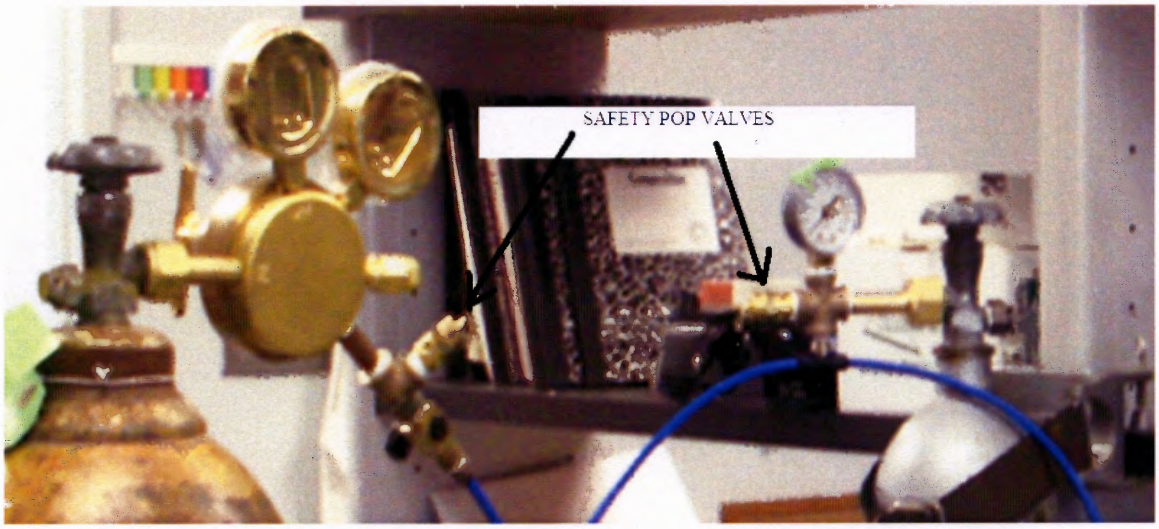

Figure 2.6 Safety pop valves to protect the VSO-EP and Series 9 valves.

2.2.5 EPX Pressure Transducer

Experimental pressure measurements will be recorded using a pressure transducer (EPX pressure transducer). The signals detected by the pressure transducer are in the magnitude of +/- 10mV to 51.91mV FSO. The EPX transducer configuration used in the "Multi Well Axonal Stretch Injury Device'' is of range 25 psi and the sensitivity is 2.0764 mV/psi. The minimum pressure measurable by the EPX sensor is ten times the cumulative noise of the system, and this must be determined using a noise meter. From observation, it is about 0.25 psi.

2.2.6 IAM Amplifier

The NI-6009 DAQ card is not capable of measuring input voltages in this range. Hence an IAM amplifier with a gain of 201.8 is used to amplify the input voltage to minimum 2V and to 10V. The safety limit for the DAQ analog input is +/- 20 V and this is well within the safety limits of the system as the peak pressure point will never extend beyond

7-10 psi, or 14 mV to 20 mV at the EPX transducer output, and to 4 V at the IAM amplifier output.

2.2.7 NI-6009 DAQ Card

All control signals and monitoring signals will be read by the DAQ card (NI-6009). The control signals include the control line from P1.2 of the DAQ card to the OEM driver, and the monitor line from P1.3 of the DAQ card to the VSO-EP valve. The software used to control the system is LABVIEW 7.1.

2.2.8 Power Supplies

Separate power supplies are used to power up the different valves and components. The VSO-EP Electronic Pressure Control Unit is powered by the 24V power supply BLP30-1024G from Power-One, and the OEM Valve is driven by the +/- 15V power supply KLT15F from Volgen.

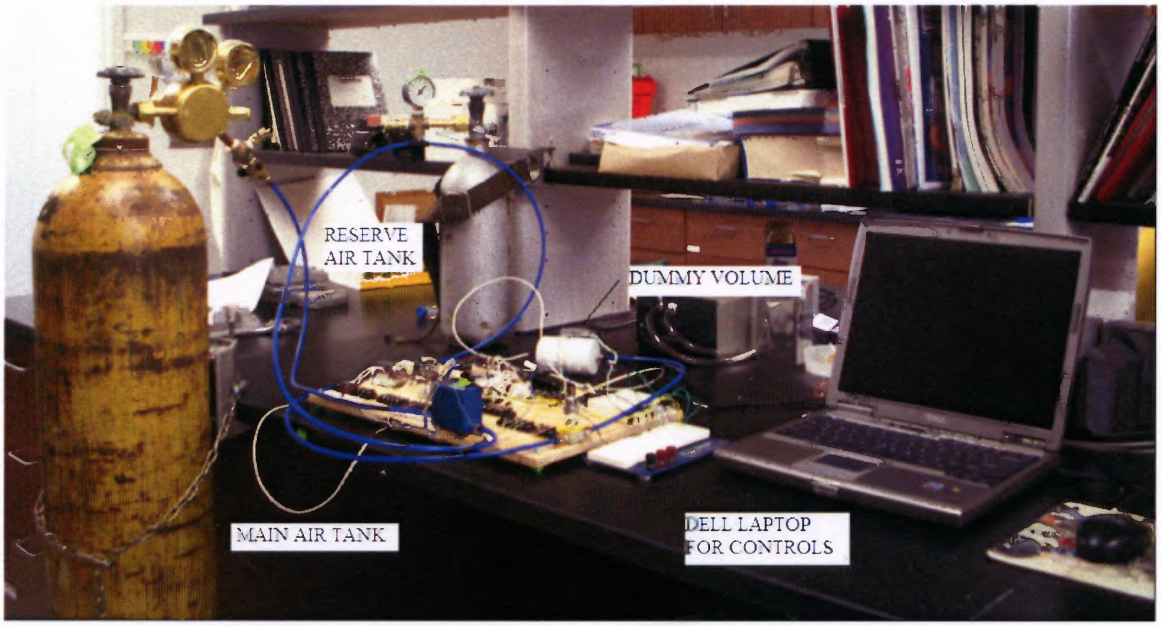

Figure 2.7 System overview.

A close-up view of the electrical circuit is also shown in Figure 2.6. For testing purposes, the DAQ I/O lines are connected to the LED's on the breadboard.

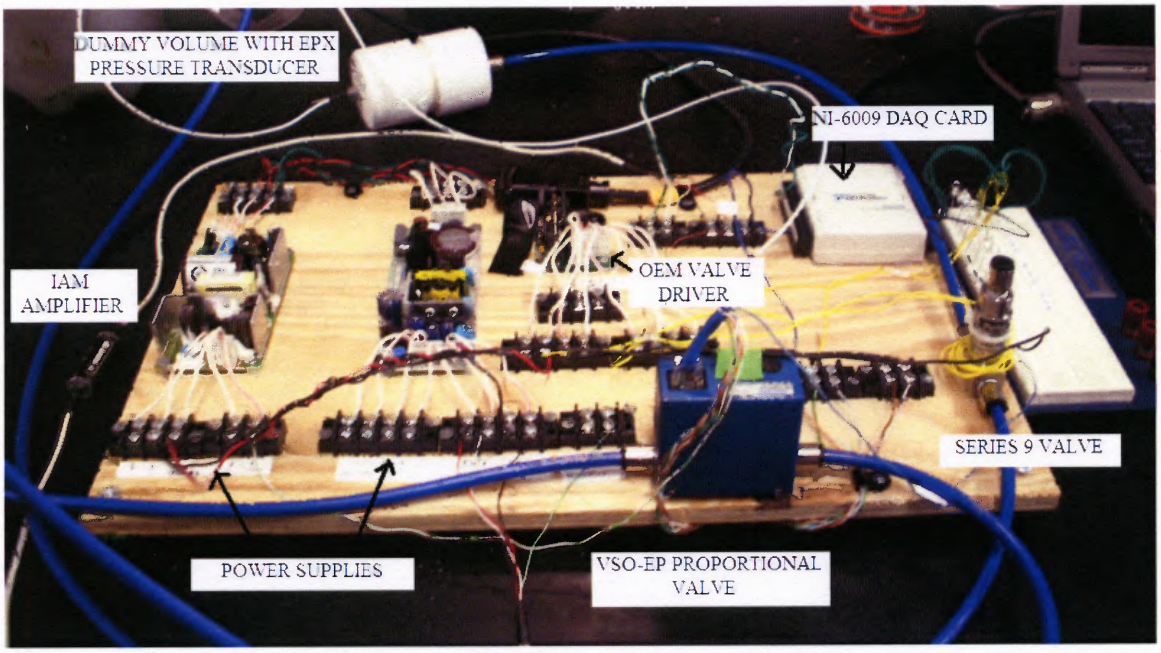

Figure 2.8 Close-up view of the control system.

2.3 Injury Device Sub-System

The mechanical subsystem consists of all the mechanical components of the system including the injury device pressure chamber, and the 24 well PEEK plate for cell culture and differentiation. The parts were designed in PRO-E.

2.3.1 Pro/E

Pro/ENGINEER (commonly referred to as Pro/E or ProE) is a 3D CAD parametric feature solid modeling software created by Parametric Technology Corporation (PTC). PRO-E is capable of creating complex 3D models, assemblies, and 2D measured drawings. PRO/E is a user friendly and efficient tool for designing and remodeling

devices. One of the features of PRO/E is that a product and its entire Bill of Materials can be modeled accurately with fully associative engineering drawings, and revision control information. It is compatible with Unix-variants, Linux and Windows. All data is interchangeable between these platforms without conversion.

2.3.2 24-Well PEEK Plate

A standard 24 well cell culture plate is designed using PEEK plastic. PEEK plastic is known for its superior durability, autoclavability and biocompatibility with NG-108 cells, and other nerve cells. Each plate has the dimensions of 3" X 4.8" X 0.75". The silicone membrane is attached the base of this plate using silicone glue for cell culture. The PEEK plate is 0.75" thick to allow adequate culture media in the plate for both growth and differentiation of NG-108 cell lines. The diameter of each well is 0.625 inch.

The PEEK plate has a groove cut along its outer edge so that it fits into the bottom frame shown above. The silicone gasket discussed above will be placed between to top and the bottom components of the pressure chamber to prevent air leaks, and allow better pressure control. Figure 2.4 is the current design of the PEEK plate.

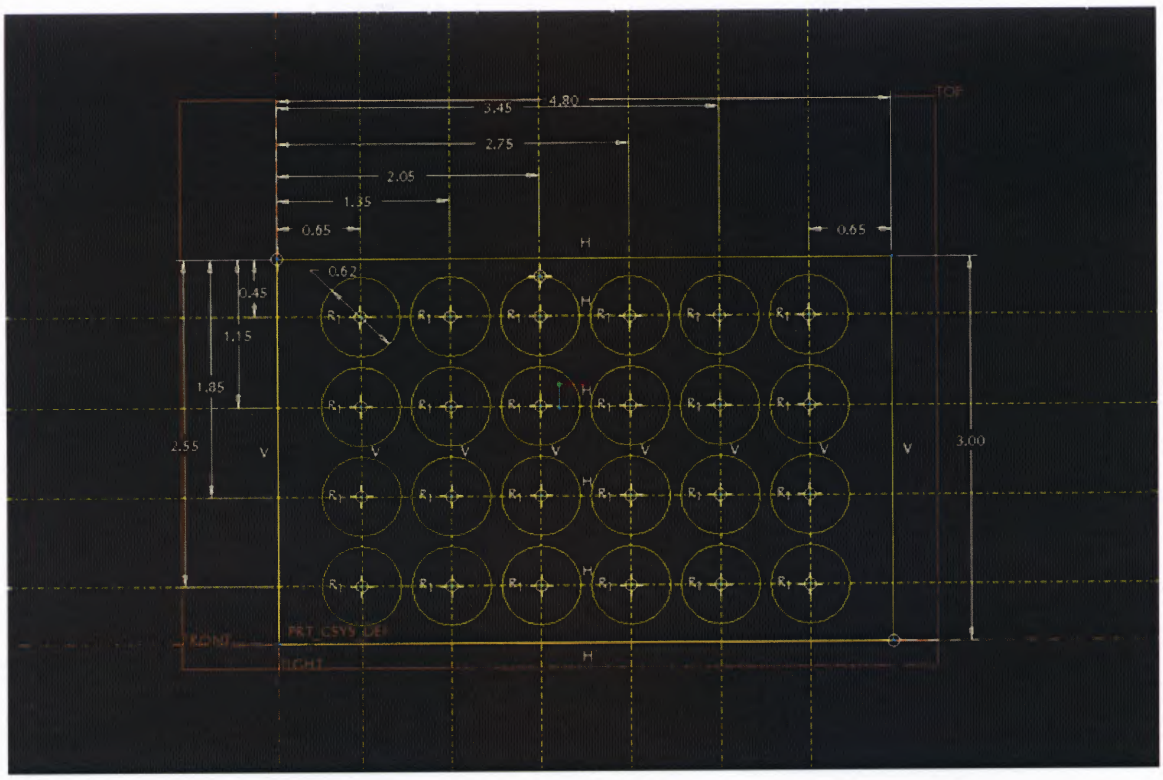

Figure 2.9 Pro/E figure of PEEK plate.

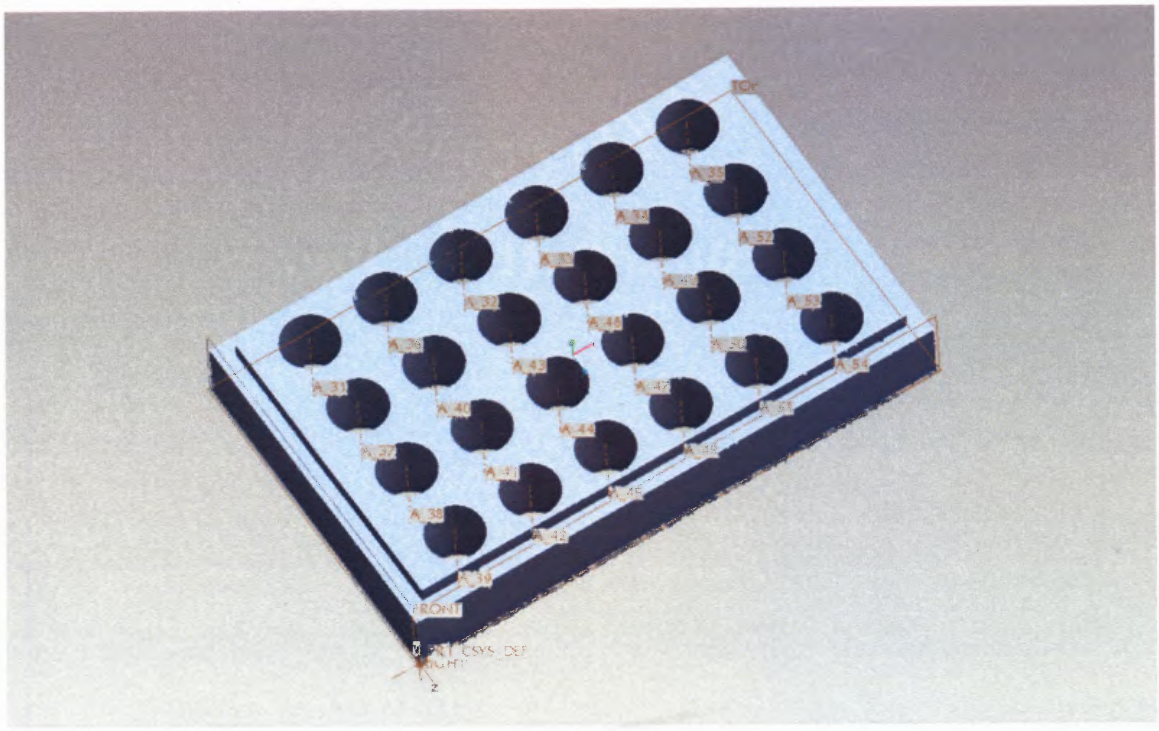

Figure 2.10 Pro/E model of PEEK plate.

2.3.3 Pressure Chamber

The 24 well plate will be subjected to a pressure pulse of 7-10 psi for 20 ms in a specially designed pressure chamber. This chamber is designed to minimize volume to enable better control of the pressure pulse, and also allow a means of measuring the silicone membrane deformation.

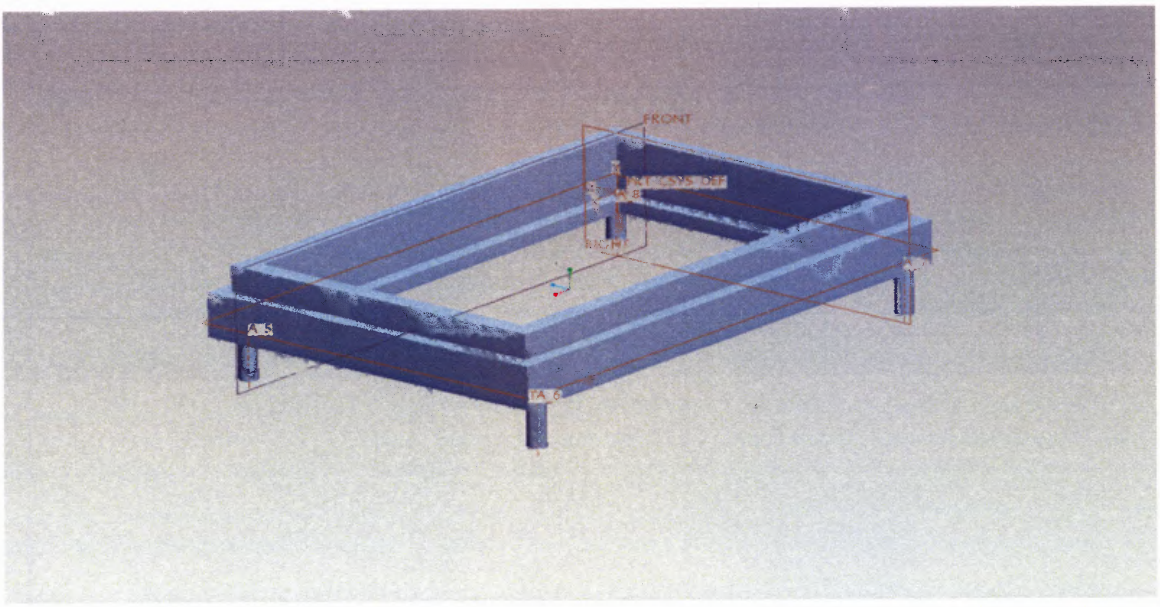

Figure 2.11 Originally designed bottom frame of Injury Device.

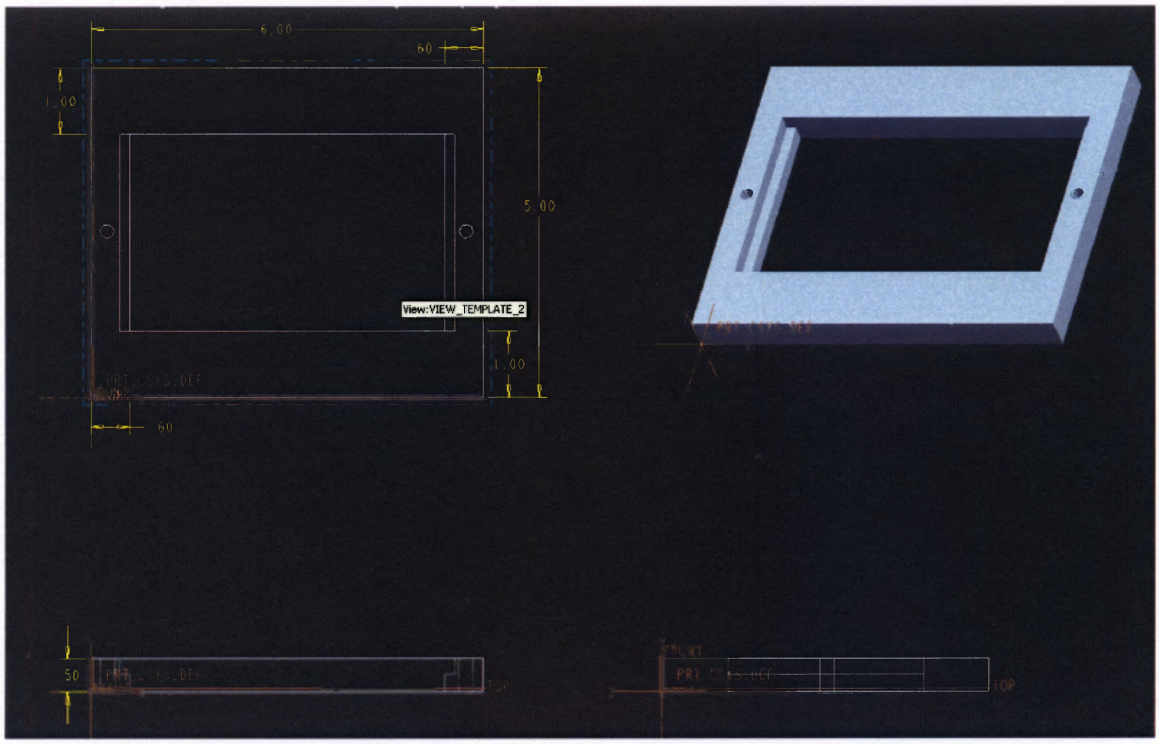

Figure 2.12 Final design of bottom frame of Injury Device.

As shown in the picture, the PEEK plastic 24 well cell plate sits in the groove with the silicone bottom protruding out of the frame to allow visual membrane deformity measurements. The top cover is then clamped onto the bottom framework using draw pins. This method is an improvement over the initial Penn model as it avoids the problems of screwing in the top lid. A silicone gasket is used to allow further air sealing.

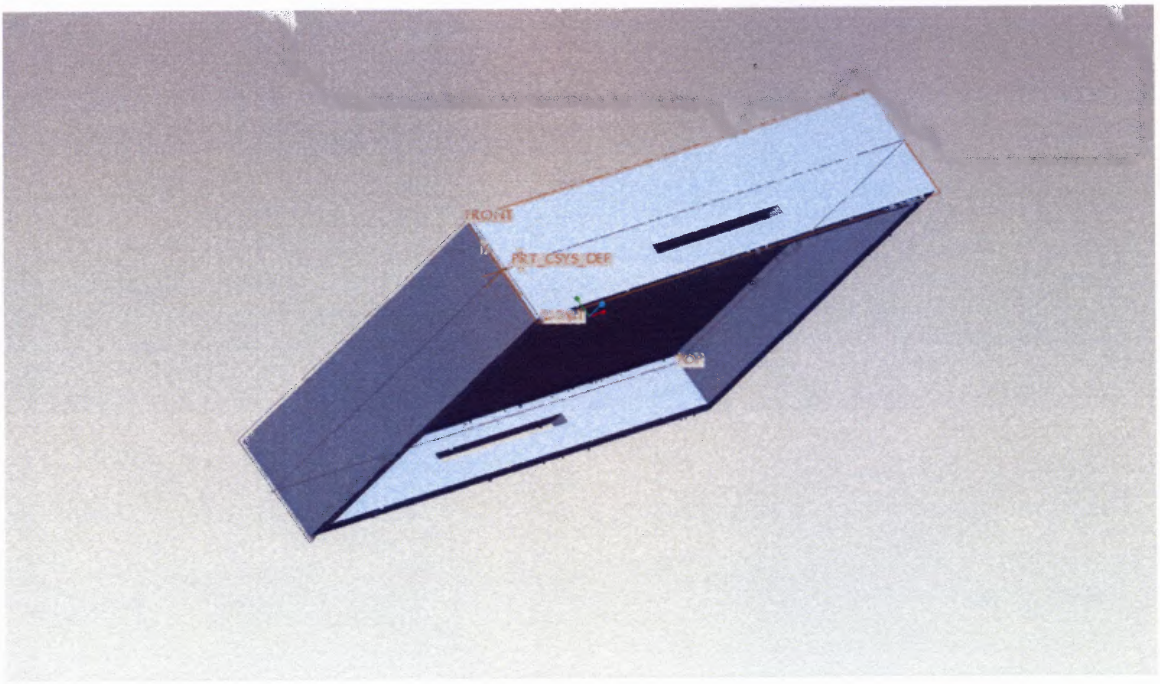

Figure 2.13 Original top plate.

Previous calculations have shown that a single pressure input localizes injury to one point only by creating localized differences in pressure throughout the pressure chamber. To avoid this problem, in our design the air enters the chamber through the four-input manifold on opposite sides of the lid as shown in Figure 2.13. By spacing out the input air supplies along either side of the lid, we ensure equal air distribution, and thereby increasing repeatability of deformation from well-to-well.

2.3.4 Final Design

The final design is based on the original designs. To maximize air flow control and minimize the excess volume a four outlet manifold of orifice size 1/8 inch is used. Other modifications in this final design include the extra pressure outlets on the top lid to measure the pressure at different points in the pressure chamber to compare uniformity

and repeatability of results. Draw pins are used to assemble all the parts together and align the model. A soft silicone gasket as shown in Figure 2.14 is used for air sealing.

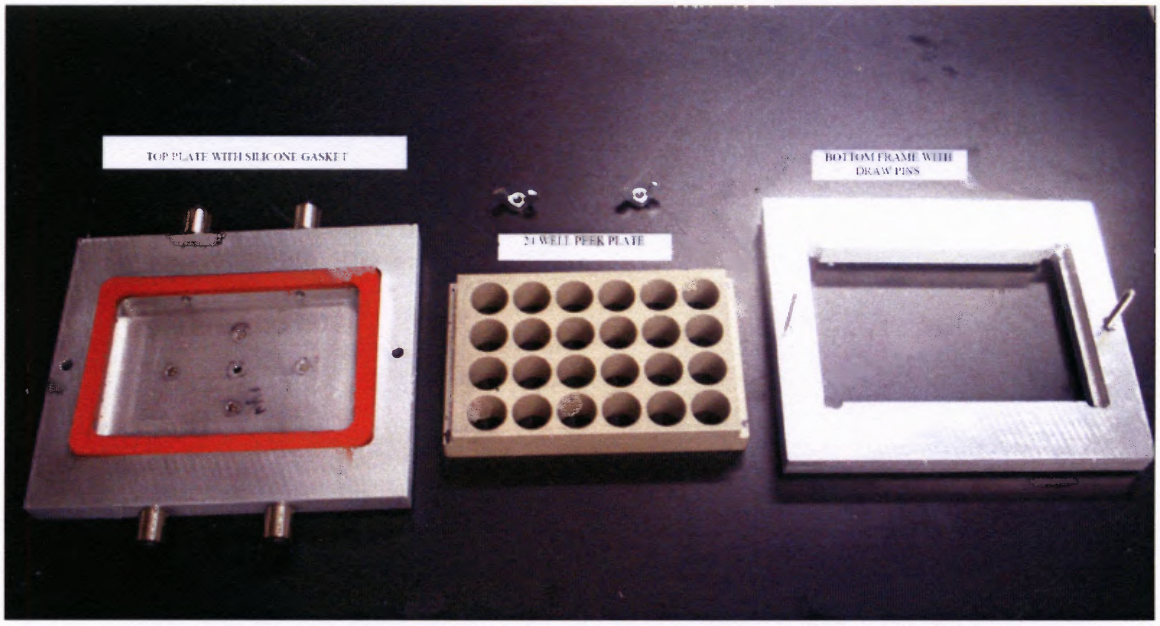

Figure 2.14 Final design of Pressure Chamber.

2.4 Biological Test Protocols

Once the design prototype is complete, the device is ready for testing and characterization. The testing phase involves tests using NG108 cell lines for biological verification. Specific protocols are followed for cell culture and differentiation as discussed hereafter.

2.4.1 NG108-15 Cell Line

The NG108-15 cell line was formed by fusing mouse N18TG2 neuroblastoma cells with rat C6-BU-1 glioma cells in the presence of inactivated Sendai virus. Specific protocols to the cell culture, and differentiation will be discussed in this section.

2.4.2 Cell Culture Protocol

The growth medium contains 90ml of Dubelco's modified Eagle's medium (DMEM), 10 ml of Fetal Bovine Serum (FBS), 2ml of Penstrip (P/S), and 1ml of HAT (0.1mM hypoxanthine, 1μM aminopterin, and 16μM thymidine). The cells are cultured in 5% CO_2 and a temperature of 37 degrees Celsius. The cells require to be passed or "split" every 3-4 days. For splitting or sub-culturing the protocol is discussed in section 2.4.2.

2.4.3 Cell Splitting/ Sub-culturing Protocol

Once the cells are ready for splitting, the following protocol is implemented.

1. Remove media from the cell culture.
2. Add 5ml Phosphate Buffer Solution (PBS) to the cell flask and leave for 2 minutes. After specified time frame, remove PBS by gently pouring it out. The PBS removes the calcium bonds so as to enable the trypsin enzyme can further remove the bonds of the cells to the ECM (Extra-cellular Matrix).
3. Add 3ml of 0.5% trypsin and wait for 3-4 minutes to allow the cells to detach from the ECM. Look under a microscope to ensure all the cells are suspended.
4. Empty out the contents of the flask into a test tube and prepare it for centrifuging using a counter weight. Centrifuge at 3000 rpm for 5 minutes.
5. A pellet of cells will be observed at the bottom of the test tube. Remove the top layer of trypsin, and discard it.
6. Add fresh media to the test tube and re-suspend the pellet. Add cells in the ratio of 1:10 to a new flask. Add 6-8 ml of growth media for further propagation.

2.4.4 Cell Differentiation Protocol

The differentiation media contains 96% Dubelco's modified Eagle's medium (DMEM), 1% Foetal Bovine Serum (FBS), 1% Penstrip (P/S), and 1% HAT (0.1mM hypoxanthine, 1μM aminopterin, and 16 μM thymidine). The following protocol is implemented for

NG108-15 differentiation. For cells to differentiate, the bottom plates need to be coated with Laminin and PLL to allow Ca^{2+} bonds to form with the extra-cellular matrix. This is a two day process as described below.

1. On the first day, the silicone wells need to be plated with 10µg/ml or 100X of poly-L lysine (PLL) Leave the solution for 1 hour.

2. Remove PLL from each well using a pipette, and leave the wells to dry for at least 1 hour.

3. Rinse wells with sterile water 3 times, and leave wells to dry overnight or refrigerate for future use.

4. On the second day, coat silicone wells with laminin, and leave it for 24 hours.

5. Remove laminin solution and rinse with PBS. Apply differentiation media when ready to plate cells.

CHAPTER 3

TESTING AND DEVICE CHARACTERIZATION

To ensure proper operation of the axon stretch injury device, the air flow characteristics will be tested. Testing of the control system will begin using a calculated 'dummy' volume identical the injury device pressure chamber and 24-well cell culture plate. The control parameters of the pressure pulse will be checked using the VSO-EP and EPX pressure transducers via the NI-DAQ interface and Labview program.

The testing phase will first determine if a constant driving force, or reserve tank pressure can be maintained by the VSO-EP proportional valve and hence determine the proper operation of the VSO-EP valve. The next test will be to ensure that the VSO-EP valve and the EPX measurements are the same. Finally, using the dummy volumes and the EPX transducer, the operation of the solenoid valve (Series 9 Valve) will be determined and verified using repeatable pressure curves.

3.1 Dummy Volume Specification

Three dummy volumes of different geometry are used for the initial testing of the system. The volume is calculated from the following final design specifications.

Diameter of each well (D): 0.625 inch

Thickness of PEEK plate (h): 0.75 inch

Width of open area above PEEK plate (t): 0.25 inch

Length of open area (l): 4.8 inch

Width of open area (b): 3 inch

$$\text{Volume} = \pi \times (d/2)^2 \times h \times 24 + l \times b \times t$$

$$= \pi \times (0.625/2)^2 \times 0.75 \times 24 + 0.25 \times 3 \times 4.8$$

$$= 9.12 \text{ cubic inches}$$

Two different geometries were created as dummy volumes: a closed cylinder of PVC tubing, and a 24 well injury plate with rigid bottoms. The latter will help to identify potential pressure differentials and the dynamics of pressure differentials relative to the geometry of the volume available.

The ideal cell culture plate volume is an exact replica of the original PEEK plate with the wells sealed. It represents an ideal PEEK cell culture plate with no leaks. This dummy volume is exclusively used to characterize the operation of the Injury Device. Figure 4.1 is a picture of the dummy volumes used by the author.

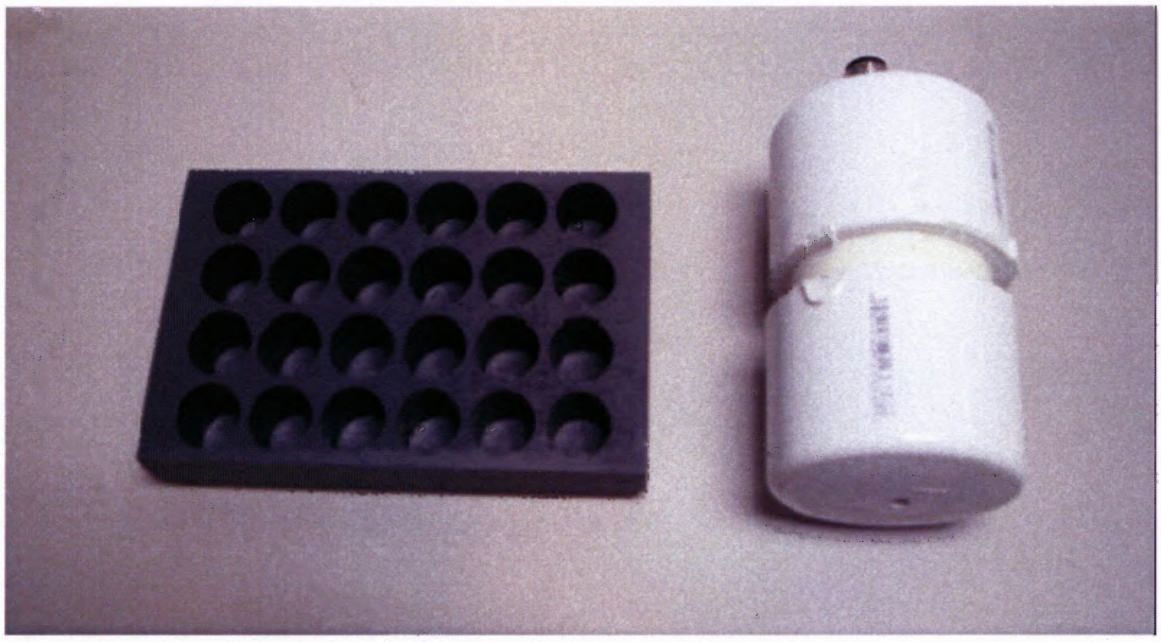

Figure 3.1 Ideal plate and dummy volume.

3.2 Calibration of VSO-EP Proportional Valve

A Labview interface developed by the author's team member Linda Chen is used to pressure up the injury device pressure chamber and the dummy volume to different pressure levels using the VSO-EP proportional valve. This code is later used to hold the pressure at a particular level to check deformity of the silicone membrane. Figure 4.2 is the Labview interface used by the author for this study.

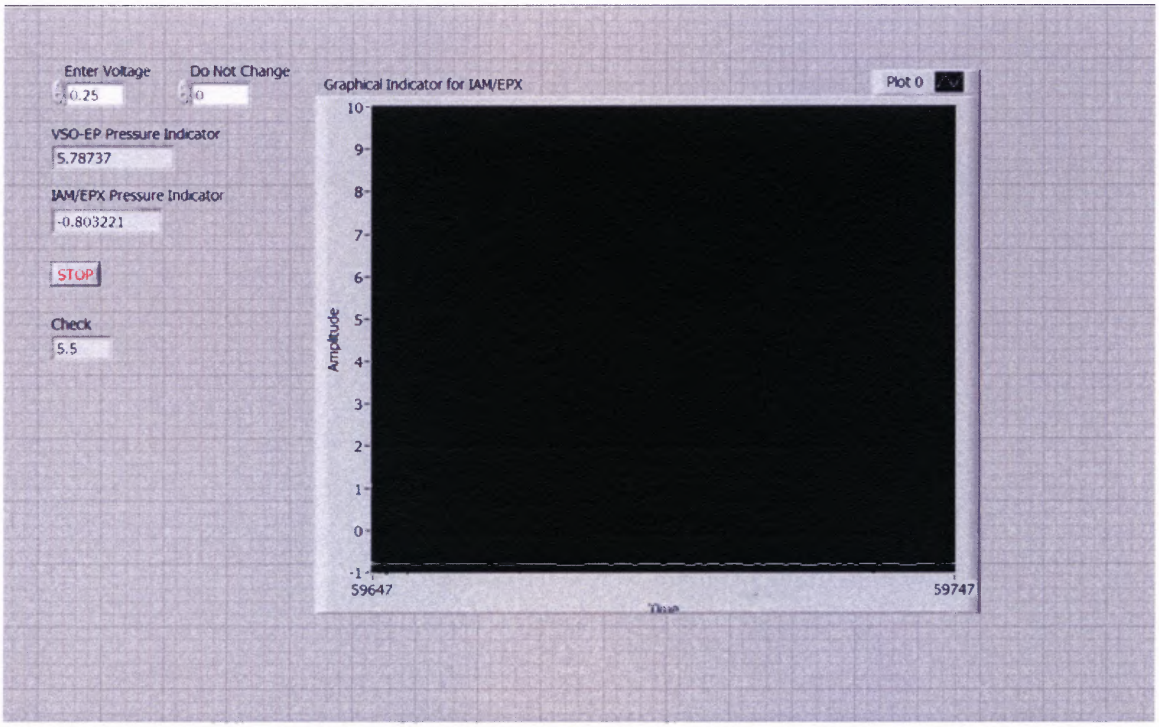

Figure 3.2 Labview interface used for pressure calibration developed by Linda Chen.

The initial calibration process for the dummy volume and the injury device pressure chamber with the ideal plate was conducted by entering different values for VSO-EP input voltage and the equivalent output of the IAM amplifier was recorded. The initial response of the voltage applied to the VSO-EP with respect to the pressure obtained by the IAM amplifier for both the volumes are shown in Figure 3.3 and 3.4.

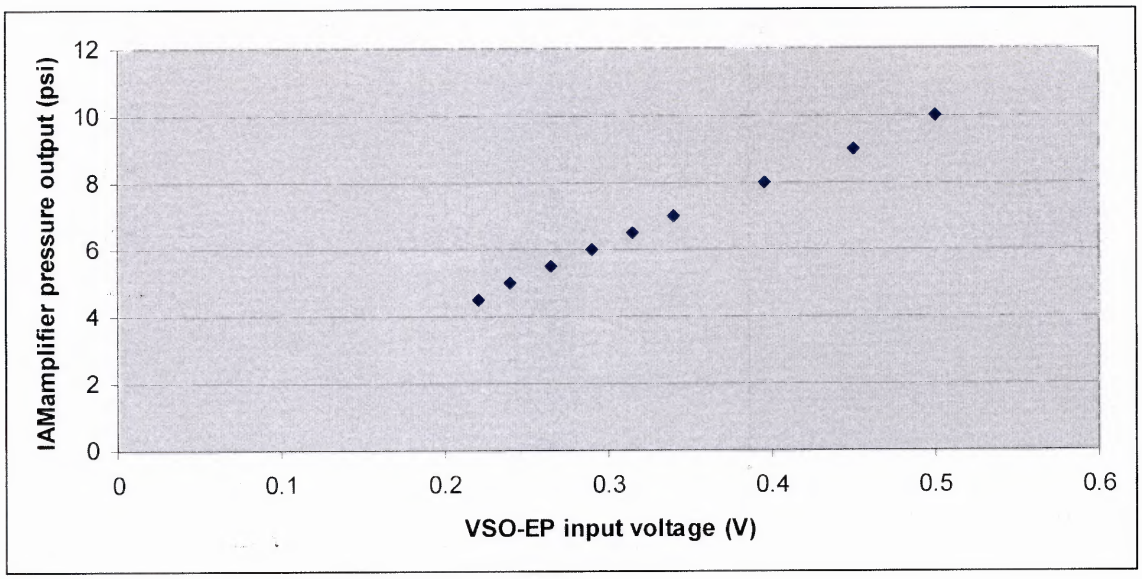

Figure 3.3 Calibration for dummy volume.

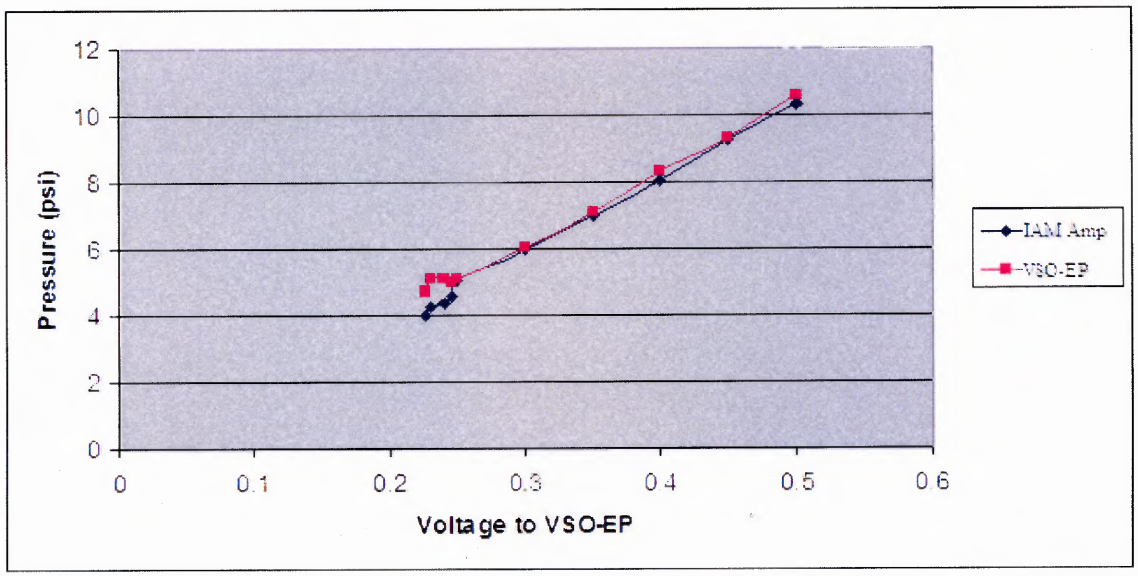

Figure 3.4 Calibration for the ideal plate..

This experiment proved that the IAM amplifier and the EPX sensor have a linear response to the pressure applied. This verifies that the parts selected by the author for this device are relevant. This experiment also proves the principle of the proportional valve where the amount of voltage applied directly controls the flow of air through it, and

reinforces the fact that the VSO-EP valve can both maintain a constant pressure in the reserve tank, as well be used for the device calibration and characterization. The pressure maintained by the VSO-EP valve can be seen in Figure 3.12.

Variations in the calibration were noticed when the ideal plate is replaced with a PEEK plate with silicone attached. This is because the silicone membrane initially attached did not have the best adhesive properties and hence caused a leaking problem. This problem is addressed by using proper gluing techniques developed by the author during this project as discussed in Section 3.3. Another way to address the leaking problem is to make slight modifications to the design of the injury device, or changing the nature of the gasket used as discussed in Chapter 4.

3.3 Silicone Membrane Attachment Techniques

Several RTV silicone glues were tested to attach he silicone membrane to the base of the PEEK plate. The three types glues tested were a elastomer Nusil MED 6015, and silicone sealants, Dow Corning RTV sealant 734, and DOW Corning RTV sealant 732 The silicone glues were selected on the basis on their viscosity, and adhesive properties.

The Nusil silicone elastomer, Part A and Part B were mixed in a proportion of 1:10. This sample has the least viscosity and thus was easy to apply but had the worst adhesive property towards PEEK plate. It had good adhesive properties for the silicone membrane though.

The Dow Corning RTV sealant 734 (a flowable formulation) was more viscous than the Nusil silicone elastomer but had better adhesive properties towards both the PEEK plate and the silicone membrane. Limited peeling off was observed for this

silicone glue. However, the silicone membrane could be easily peeled off when the Nusil elastomers were used as shown in Figure 3.23.

The best result with respect to adhesive and sealant properties was the Dow Corning RTV Sealant 732. However it was the most viscous of all three glues. A specific technique is used to apply this glue to the PEEK plate and then attach it to the silicone membrane as described further in this section.

The best way to apply the Dow Corning RTV Sealant 732 onto the PEEK plate was using the sponge tips as shown in Figure 3.5. Other techniques tested and rejected were using a stiff paint brush and the synthetic roller as also shown in Figure 3.5. The roller did not spread the glue evenly and caused accumulation of silicone glue in the wells of the PEEK plate. The paint brush worked better than the roller, though the bristles were not hardy and kept coming off on the silicone glue. Hence the sponge tips which were small and easy to use were the best tool.

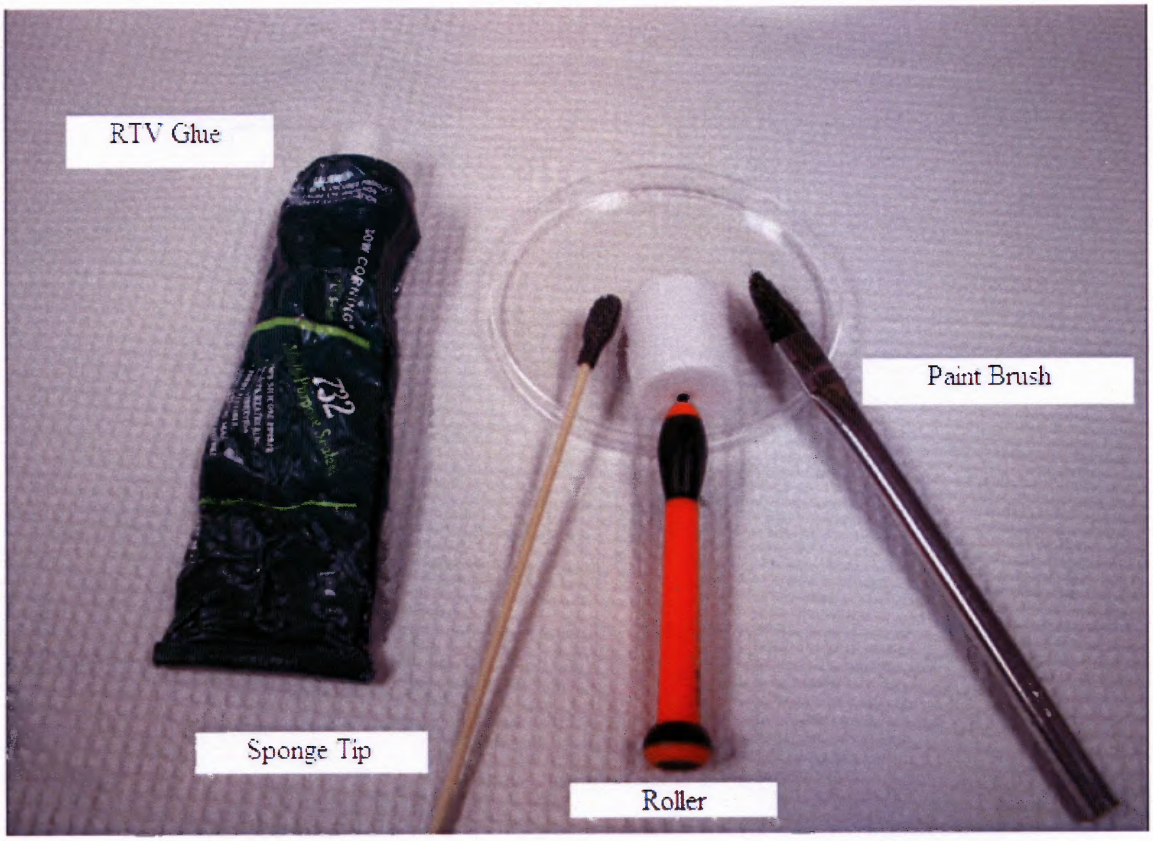

Figure 3.5 Glues and techniques.

Once the silicone glue is applied to the PEEK plate, the silicone membrane is attached using a specially designed technique to avoid air bubbles from being trapped between the membrane and the PEEK plate. Air bubbles are responsible for inadequate membrane attachment and leaking problems.

Figure 3.6 shows the components of the membrane attachment system developed by the author. The silicone membrane is first laid out on the lower frame as shown in Figure 3.7. The top frame is then attached to the lower frame using clips to fix the membrane as shown in Figure 3.8. This frame is then stretched over the High Density Poly Ethylene (HDPE) block as shown in Figure 3.9 to avoid any air bubbles being trapped and fastened with two more clips on the posts. The PEEK plate with the silicone

position is maintained by the stoppers along the PVC block as shown in Figure 3.10. A weight is put on the PEEK block to ensure maximum adhesion.

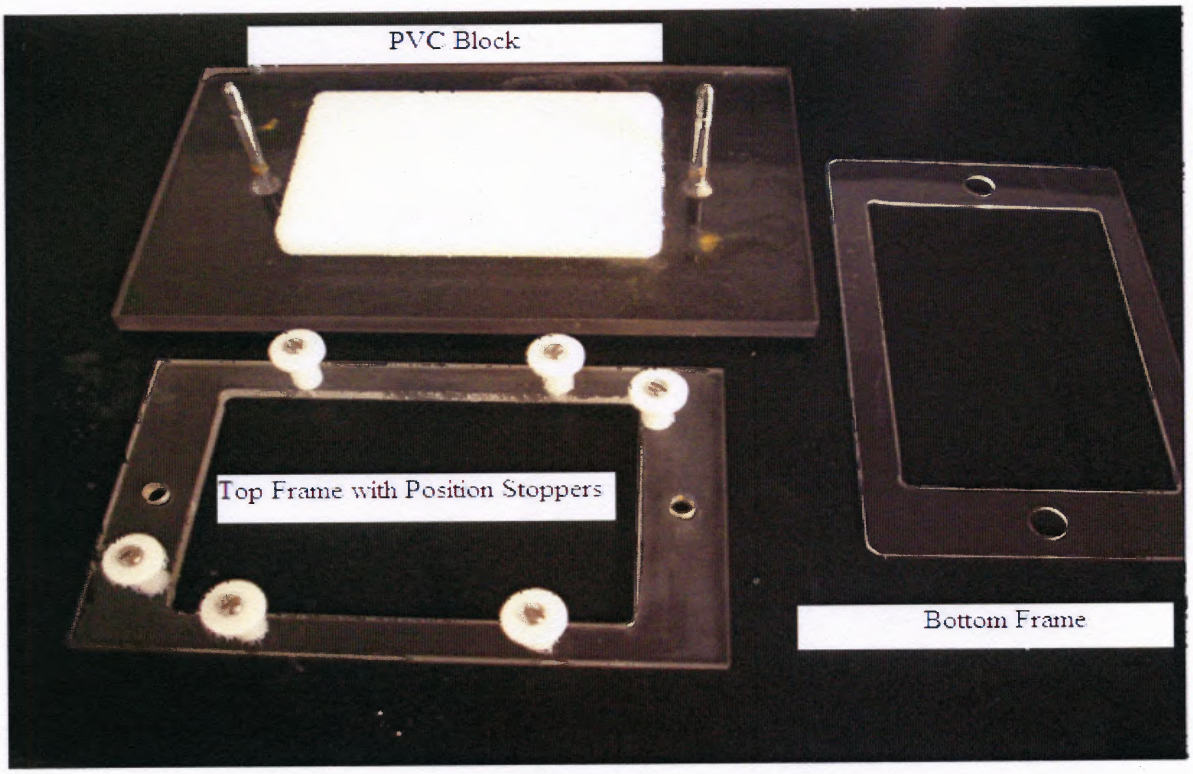

Figure 3.6 Components of the silicone attachment system.

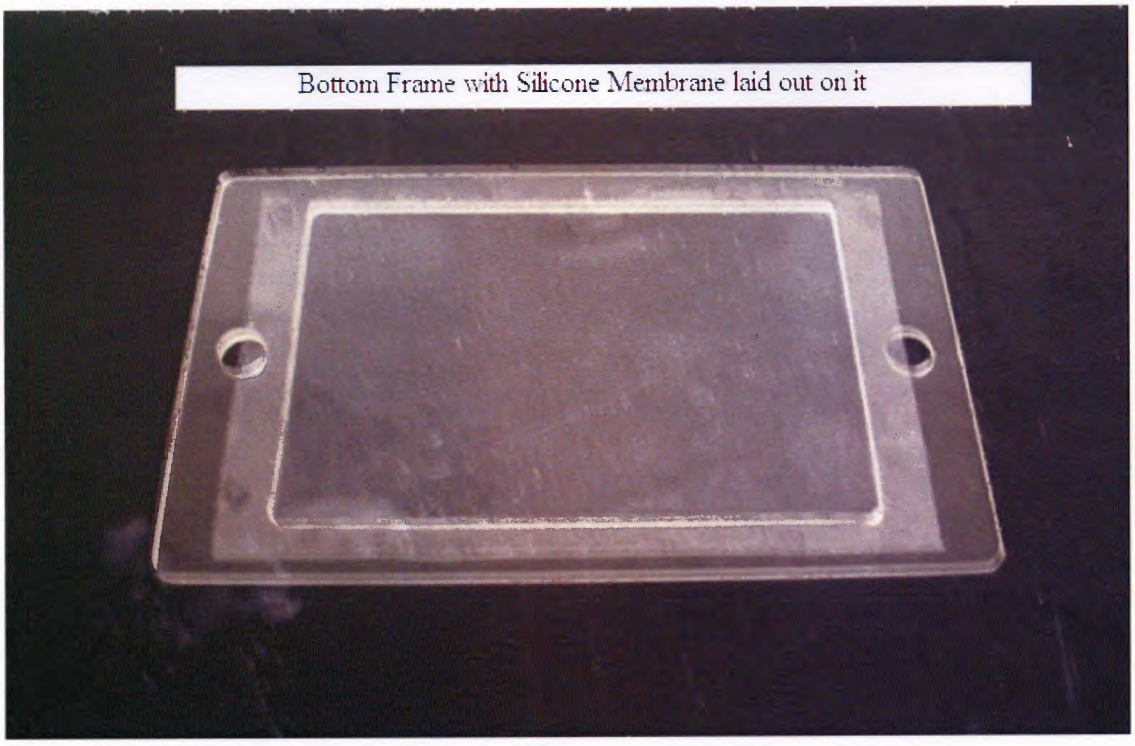

Figure 3.7 Bottom frame with silicone membrane laid out on it.

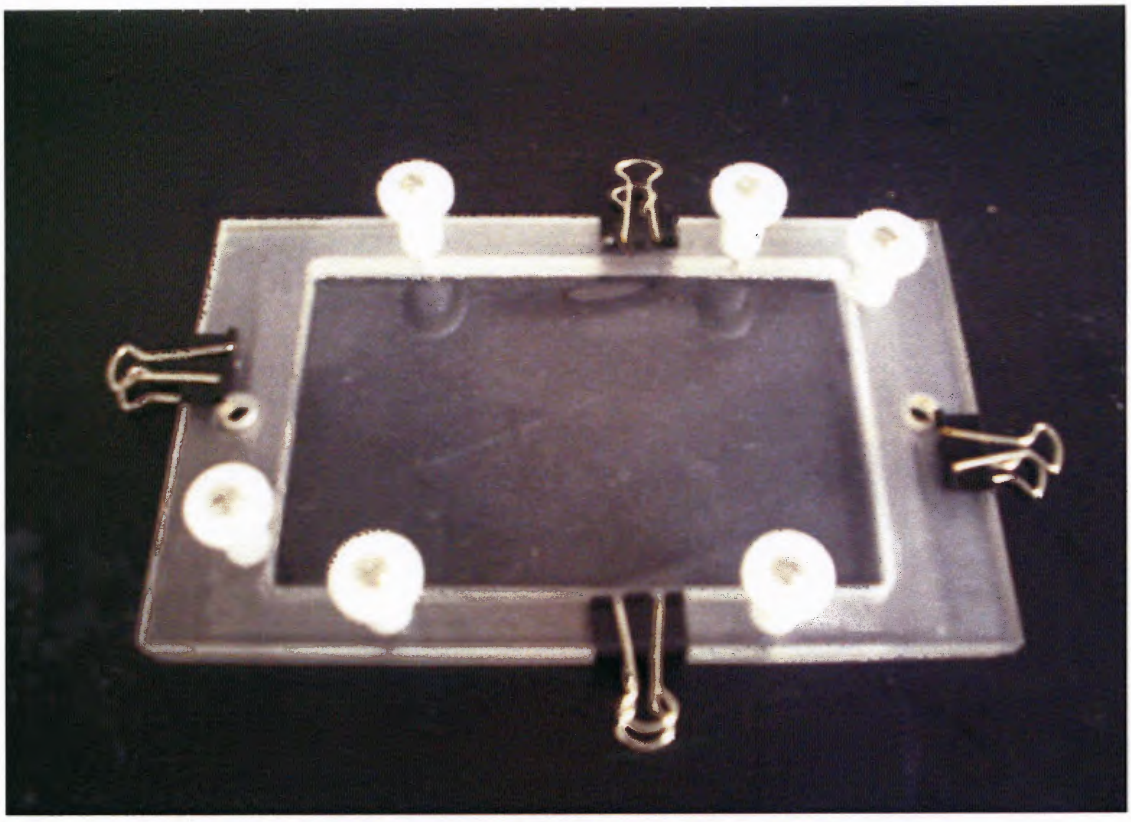

Figure 3.8 Silicone membrane frame.

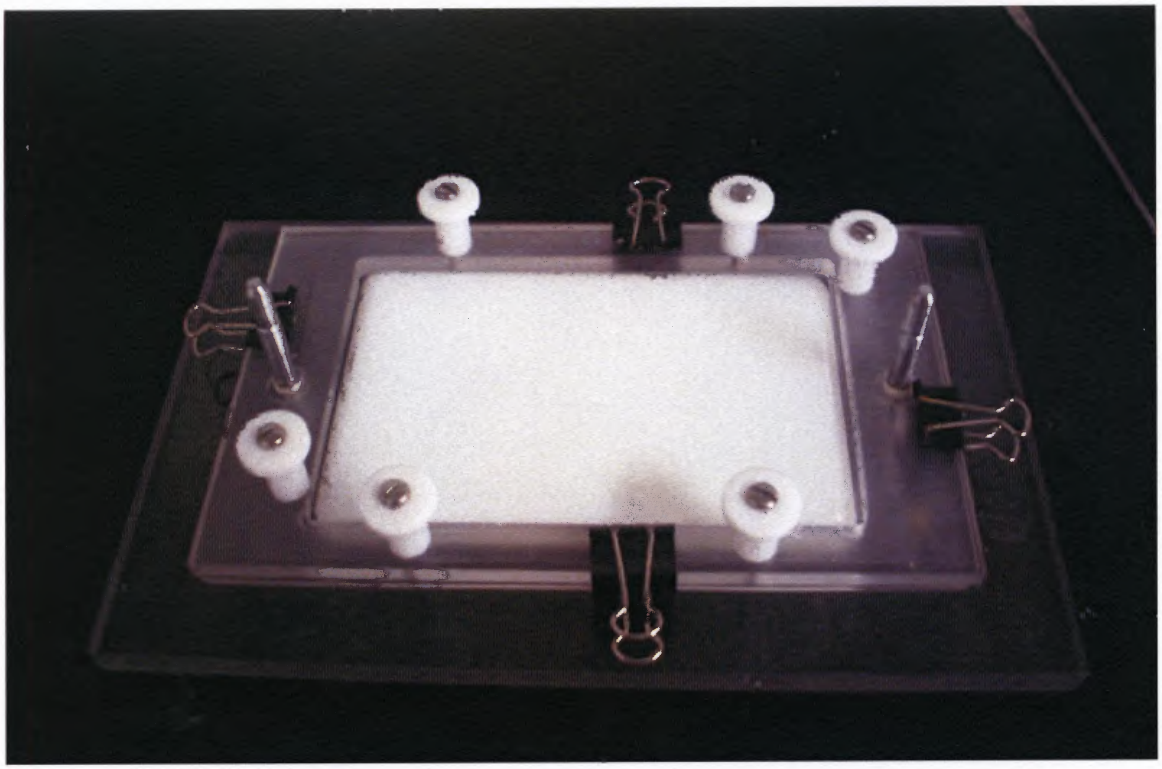

Figure 3.9 PVC block with stretched silicone membrane.

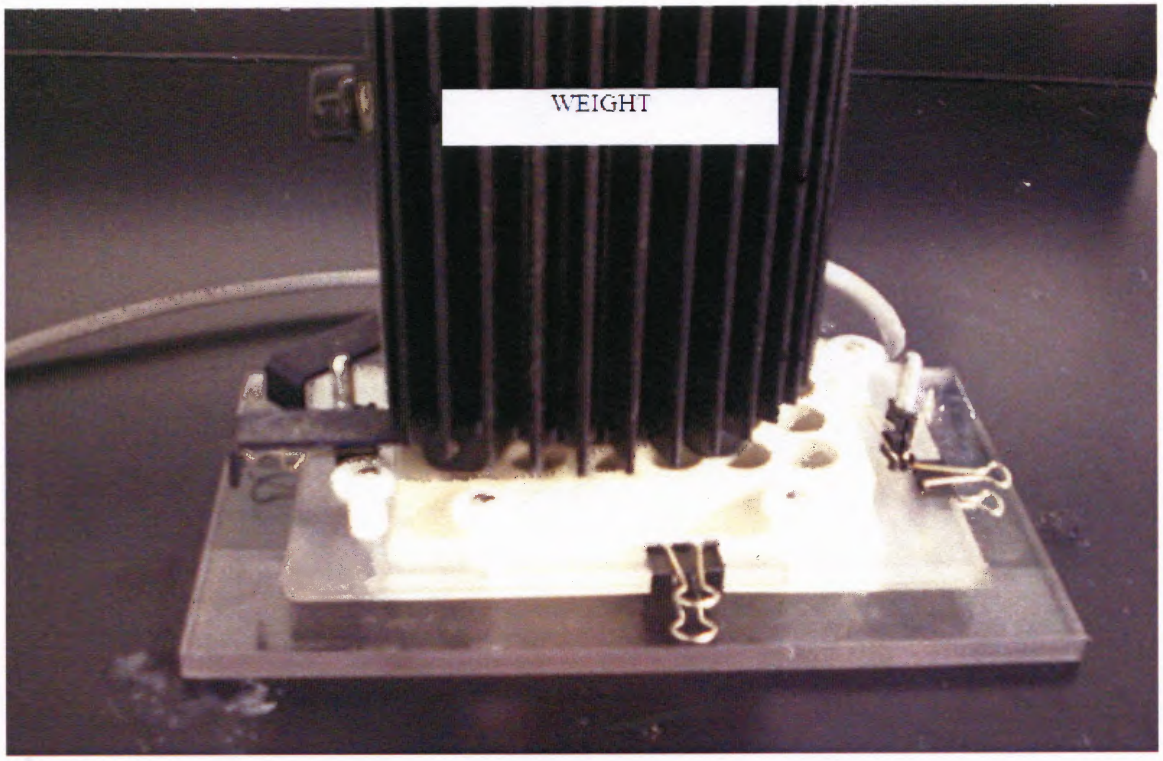

Figure 3.10 Final silicone membrane attachment setup.

Few problems encountered in this methodology were that the process could be tedious and more significantly, the PVC block must be at least 2 mm wider than the PEEK plate on all sides to allow uniform attachment of the membrane to all the edges. In this model the PVC block was found to be slightly shorter along the width of the PEEK plate. To overcome this and test the hypothesis, the author conducted the same experiment on a plain counter top. This experiment was remarkably more successful than the block model even though it did not completely eliminate air bubbles trapped within the surface. Figure 3.11 shows the improvised setup used to test the hypothesis.

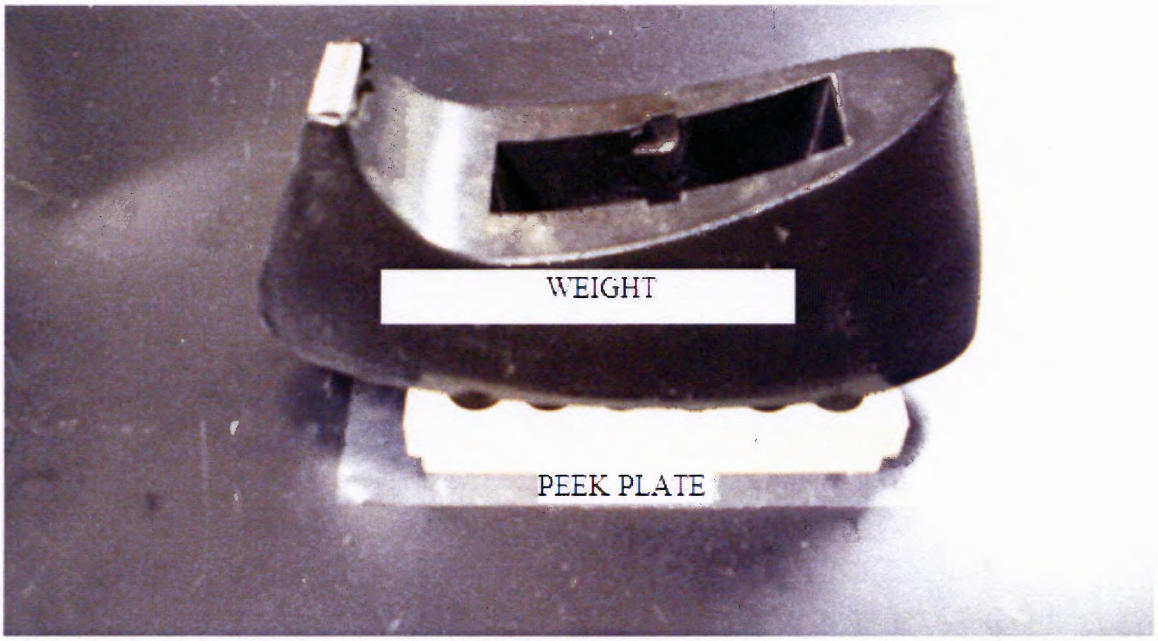

Figure 3.11 Improvised version of silicone attachment setup.

3.4 Pressure Response of Injury Device Pressure Chamber

A number of experiments were conducted to test the pressure response of the Injury Device. The most important criteria the author checked for was uniformity of flow of air throughout the Injury Device Pressure Chamber and hence the repeatability of results.

This can be done by pressuring up the chamber to 7 psi or less and individually monitoring the pressure curve in each of the nine locations shown in figure 3.12.

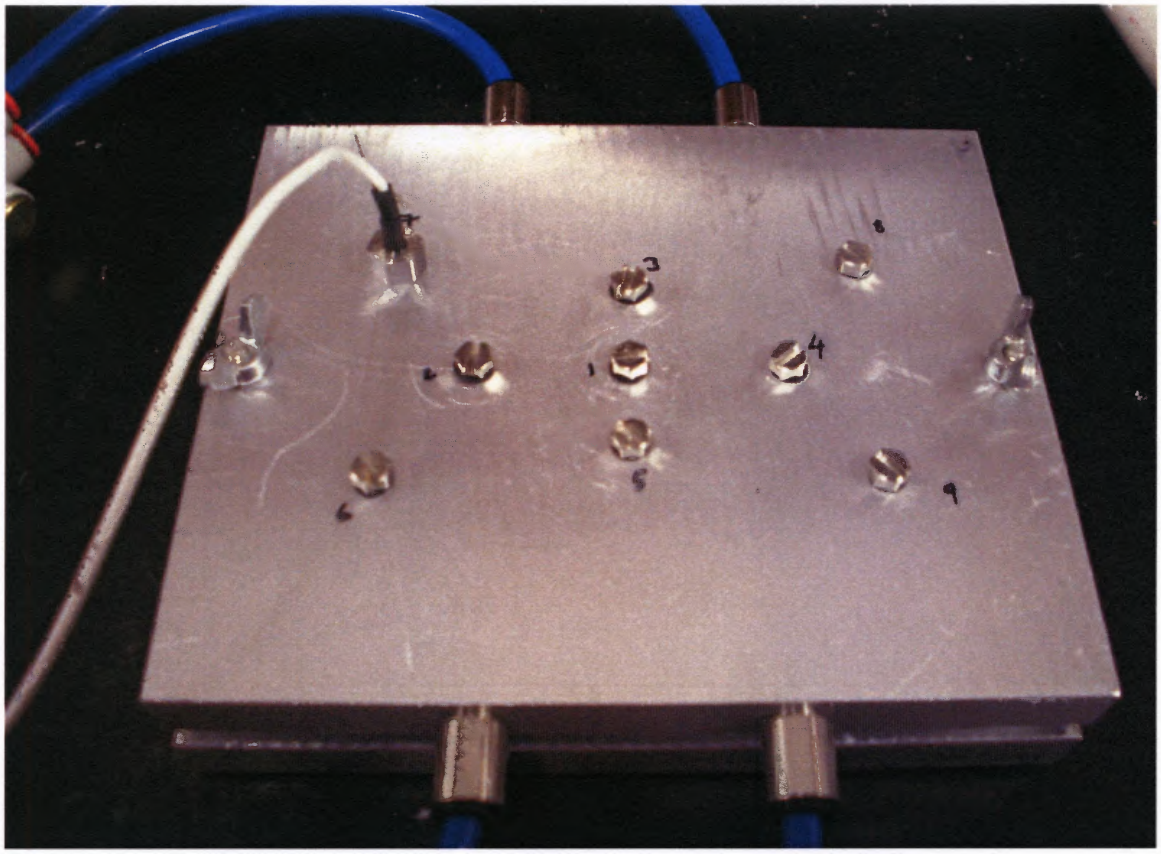

Figure 3.12 Nine locations to monitor pressure response of the device.

The Labview interface developed by Linda Chen is used to check the "spike" response in each of the nine locations. Repeatable results were obtained for all the five locations confirming that the air flow within the Injury Device was uniform. Slight offsets were observed in some of the responses and found to be dependent on the positioning of the EPX pressure transducer in each location. The results obtained from this experiment are shown in Figure 3.13 to Figure 3.14.

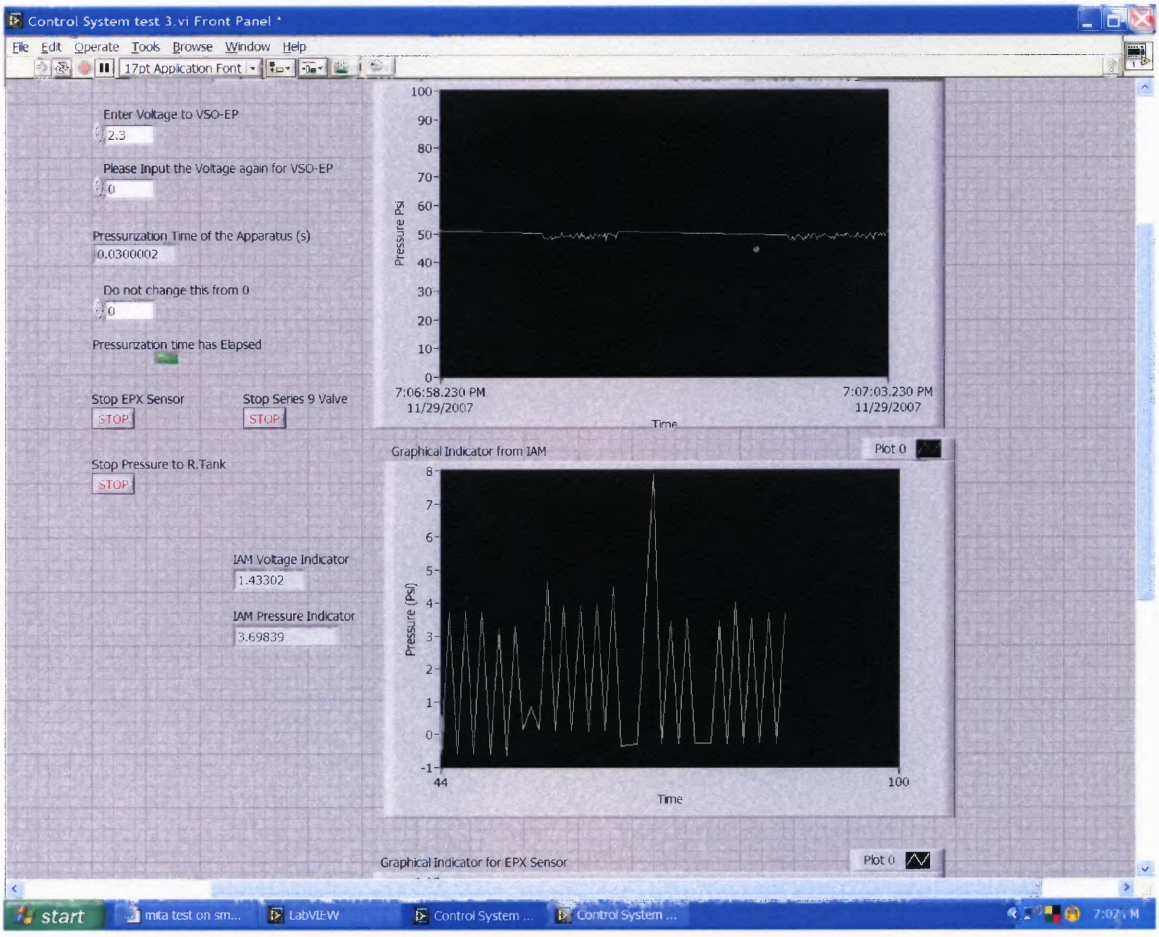

Figure 3.13 Position 1 at 40 psi in reserve tank.

Figure 3.13 shows that the data displayed by Labview waveform generator obviously has some limitations. From the results obtained in this section, one of the drawbacks in these waveforms obtained from Labview is that the downward slope is not captured. The author discovered that the sampling rate of the Labview waveform generator is not high enough to capture all the data points and hence the data collected needs to be stored in a buffer before being shipped into the waveform generator. Future versions of the Labview code need to implement the storing of all the data points in a buffer to overcome the missing data points problem. The data was also recorded in MS

sample of data collected at position 1 for six samples to record more data points from the experiment as shown in Figure 3.14.

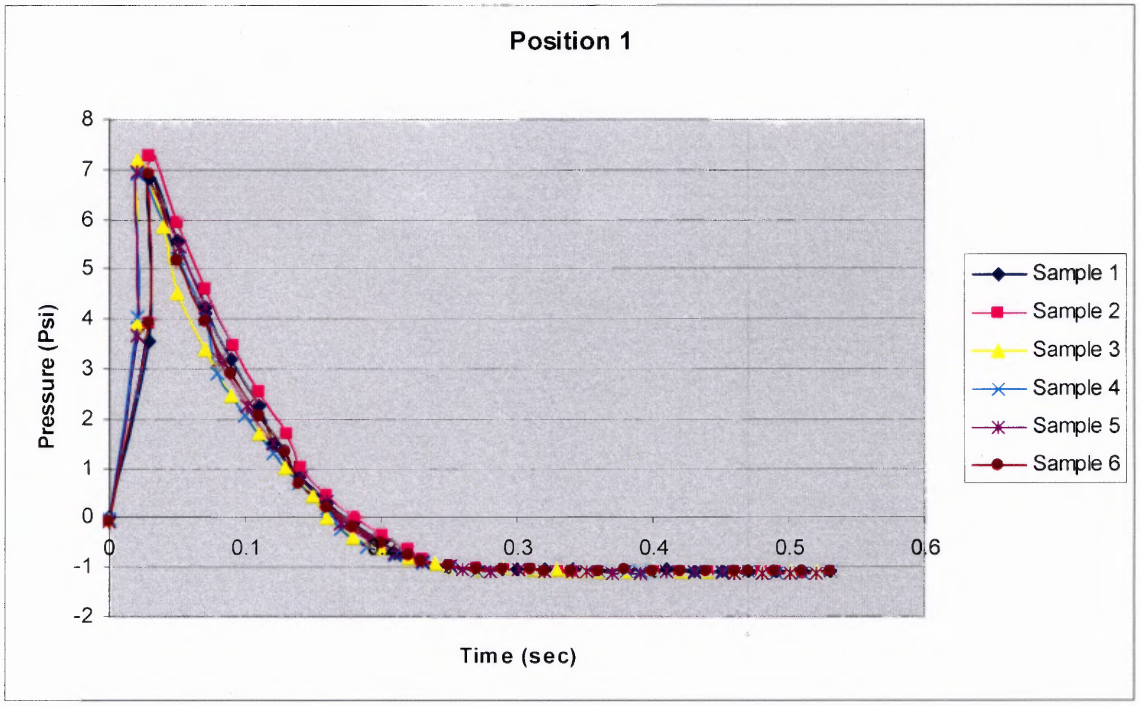

Figure 3.14 Data recorded in MS Excel for one pressure pulse of 20 ms peaking at 7 psi.

Another method used to determine uniform distribution of air in the injury device was by randomly selecting a sample of data collected from positions 6,7,8,9 and 1 as they are spread out around the chamber. The graph shown in Figure 3.20 proves that air distribution was uniform around the entire injury device pressure chamber.

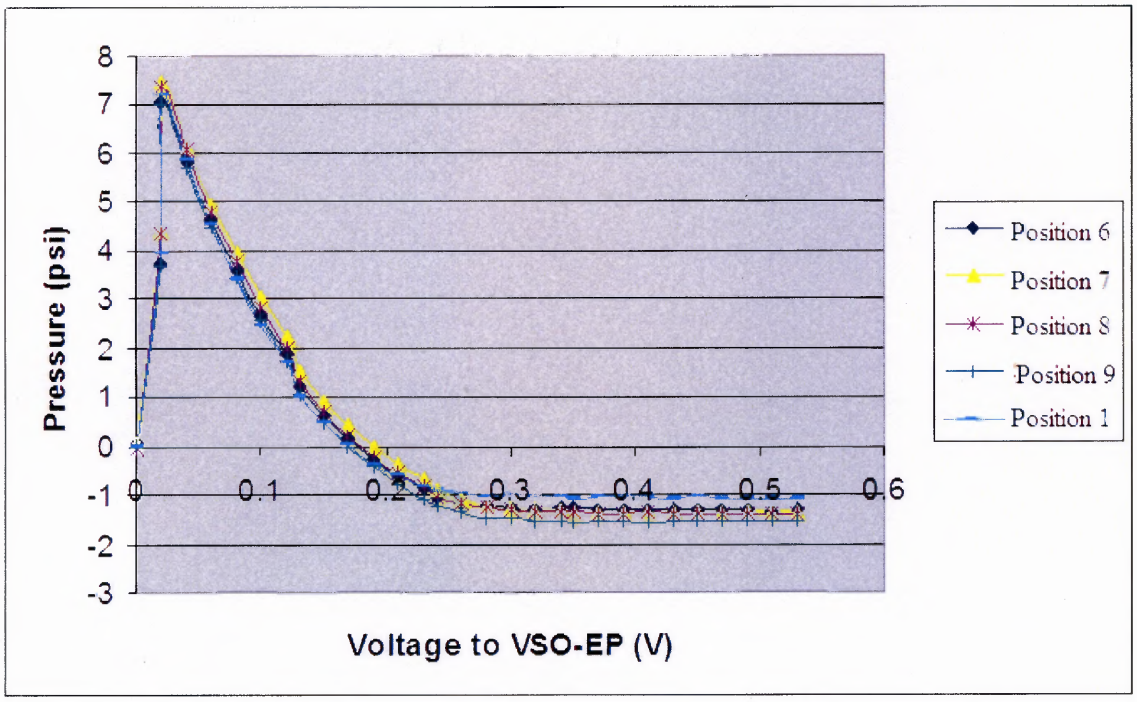

Figure 3.15 Comparison of pressure pulse at locations 6, 7, 8, 9 and 1.

The other methodology used to confirm the uniformity of the air flow is using the initial Labview interface described in Figure 3.19 to hold the pressure at a certain level to measure the strain on the membrane. As shown in Figure 3.21, there is uniformity in stretch of the membrane wells throughout the 24 well PEEK plate.

As the silicone membrane gets stretched, the maximum pressure required to pressurize the chamber is lower than the ideal plate. The graph in Figure 3.17 shows multiple deformations in one test PEEK plate with silicone membrane attached to it. There is obviously a difference in the static and dynamic characterization of the PEEK plate and this problem needs to be addressed using better deformation measurement techniques.

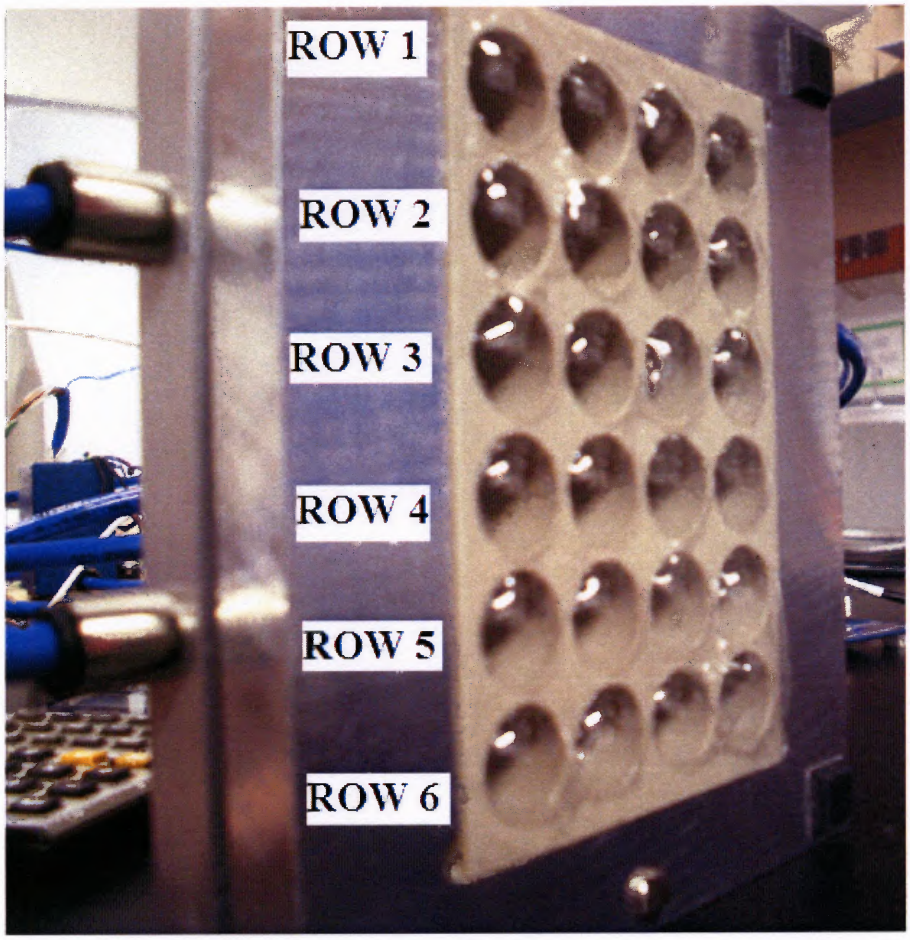

Figure 3.16 Silicone membrane under stretch analysis.

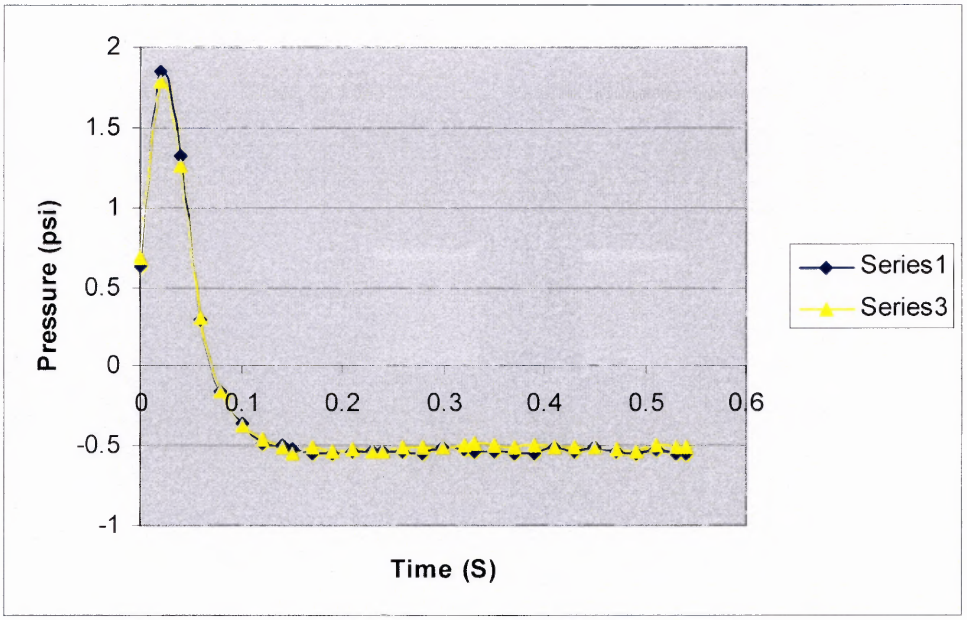

Figure 3.17 Pressure pulse detected in test PEEK plate with silicone membrane at 40 psi

3.5 Silicone Gasket Test

Another techniques developed to control the leaking problem is testing the gasket used in the study. Different silicone gaskets were developed using Nusil silicone glue and mixing the two parts of the glue in three different rations 1:10, 1:7, and 1:5 to create silicone sheets of varying durometer. The setup of this experiment is shown in Figure 3.23.

Figure 3.18 Study of silicone gaskets.

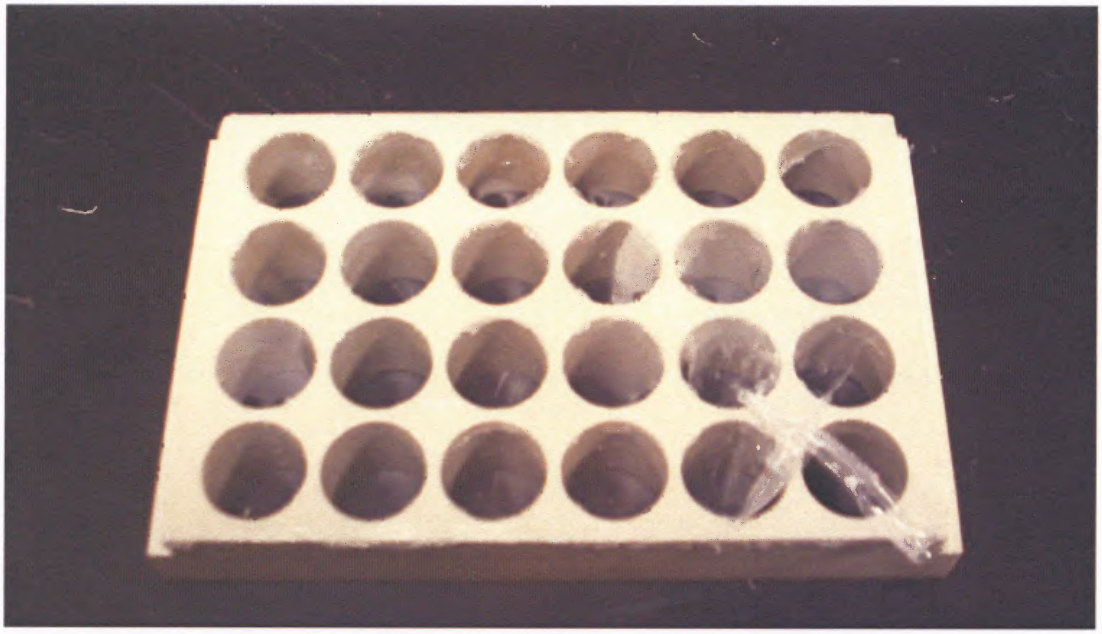

Figure 3.19 Result from Nusil elastomer test to stick silicone membrane on PEEK plate.

From this study, no significant difference was observed for different silicone rings. The conclusion from this experiment is that using a round gasket instead of a flat one may be more beneficial.

CHAPTER 4

RESULTS AND CONCLUSION

Air leaks encountered in this study prove to be the major hindrance is developing an efficient, repeatable, and reliable device. The problem has been tackled in several ways, starting with testing different gluing techniques, and using different silicone gaskets.

To improve the device and prevent possible air leaks we plan to introduce a mask which can be screwed into the PEEK block to contain the air pressure and the culture liquids to each well. Figure 4.1 is a futuristic model of this design.

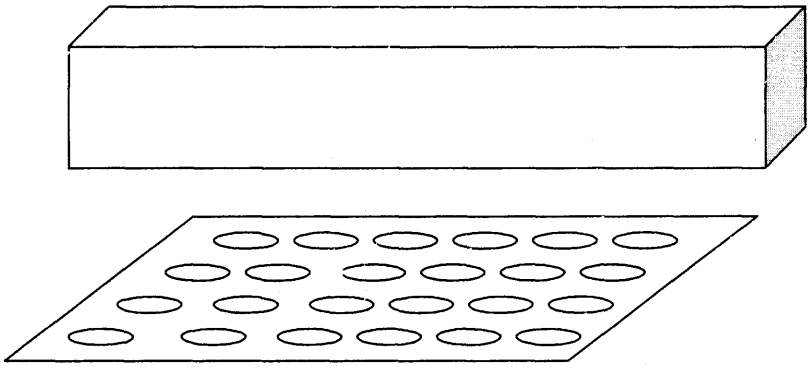

Figure 4.1 PEEK plate with mask.

Another way to contain the air leak is to build an in-built gasket both along the top edge as is the case in the current model, as well as the bottom groove as originally designed by the author. Using a circular gasket with higher durometer can also limit the air leaks from the system as a circular gasket has higher compressibility than a flat gasket as is used in the current model.

Initial biocompatibility studies in this project have shown superior biocompatibility between the PEEK plastic and NG108 cell lines. NG 108 cells were

cultured in growth media and later in differentiation media on the silicone membrane placed in the PEEK cell plate for 3 days. The cells seem to thrive well in this environment. Figure 6.1 is a picture of NG 108 cultured and differentiated in the PEEK multi well plate after 3 days.

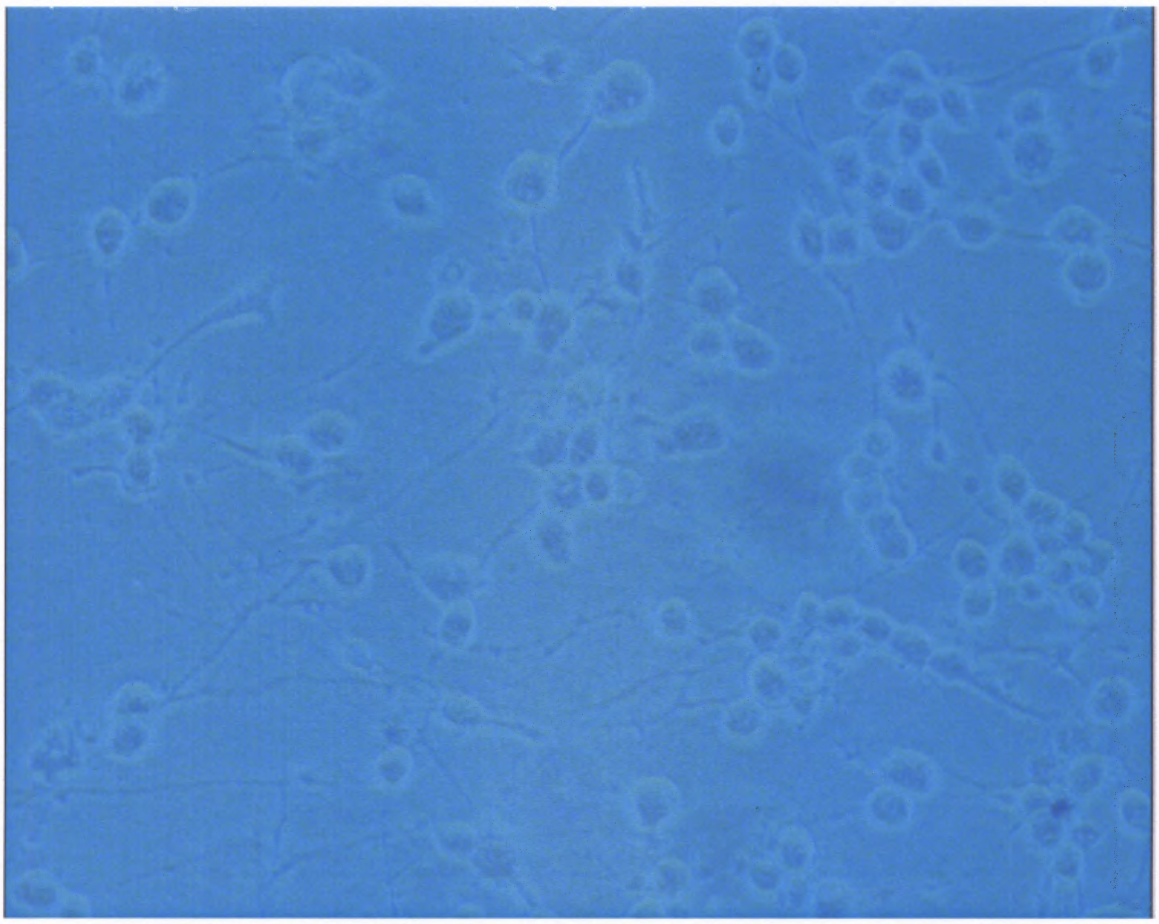

Figure 4.2 Differentiated NG108 cells in PEEK plate with silicone membrane.

Another preliminary test conducted on the silicone wells was the feasibility of using 0.5 μm fluorescent microspheres to allow future biological viability tests. A 100X concentration of fluorescent beads was tested for their properties on silicone membrane. Figure 4.3 shows the results obtained from this experiment. Other concentrations tested were 1000X, 10000X, and 100000X. The 100X concentration gave the best results.

concentration of fluorescent beads was tested for their properties on silicone membrane. Figure 4.3 shows the reslts obtained from this experiment.

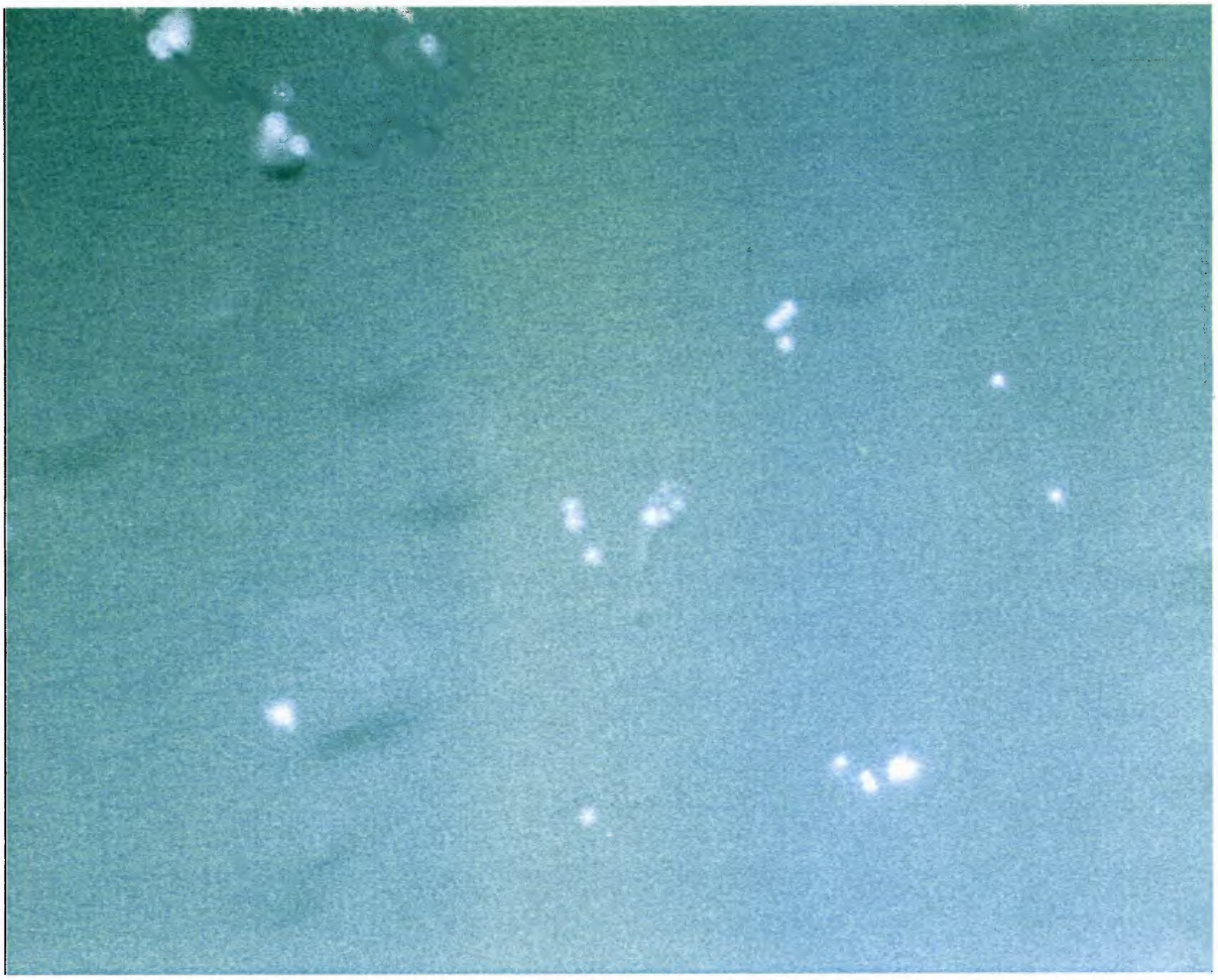

Figure 4.3 Fluorescent microspheres attached to silicone membrane for future testing.

CHAPTER 5

FUTURE WORK

In this project, my endeavor is to create a high throughput, cost effective, and user friendly, *in vitro* model for uni-axial stretch of neurons to simulate the effect of TBI, in particular uni-axial stretch in on the neurons of the brain. Future work can include a more extensive well-to-well study on repeatability of strains and strain rates. In this prototype, NG108 cell lines are primarily used for experimentation. Future studies on cortical cells, or astrocytes can better predict and simulate the effect of uni-axial stretch injury.

With respect to the device itself, using clamps instead of draw pins will be a better approach to get the same sealing every time. This would avoid the problem of screwing in the draw pins to ensure the device is air tight.

Better methods of tracking the strain and the strain rates real-time can also be another scope for future work. For example, using a window on the top plate to physically measure the deformation of the membrane in the un-deformed and the deformed states can further test the deformation hypothesis.

For further static measurements, a five point study of the strain vs pressure applied characteristic can be conducted for 5 plates with 24 wells each. The five pressure points are already drilled into the top plate. Future studies can include a well-to-well study for each of the 24 wells. The amount of strain induced may be visually calculated using the Cauchy Green equation using the fluorescent marker method [14]. The variance from well to well will then be calculated using statistical tools like the Student t test to prove the hypothesis.

After the differentiated cells are subjected to the deforming air pulse, another study using live-dead assays can be used to determine the uniformity of the stretch injury using Invitrogen Flourospheres. This study would give a biological viability result to further characterize the device.

REFERENCES

1. Center WRAM. Traumatic Brain Injury Program. *Walter Reed Army Medical Center* [Website]. Available at: http://www.wramc.amedd.army.mil/departments/Aasc/new/brain.htm. 2006.

2. NRG Networks. Traumatic Brain Injury. *NRG Networks* [Website]. Available at: www.tbiinfo.com. 2001.

3. Bernstein DM. Recovery from mild head injury. *Brain Inj.* 1999;13(3):151-172.

4. Brain Injury Association. The Costs and Causes of Traumatic Brain Injury. [Website]. Available at: www.biausa.org/costsand.htm. 2001.

5. Rimel RW, Giordani B, Barth JT, et al. Disability caused by minor head injury. *Neurosurgery.* 1981;9(3):221-228.

6. Alexander MP. Mild traumatic brain injury: pathophysiology, natural history, and clinical management. *Neurology.* 1995;45(7):1253-1260.

7. Guerrero JL, Thurman DJ, Sniezek JE. Emergency department visits associated with traumatic brain injury: United States, 1995-1996. *Brain Inj.* 2000;14(2):181-186.

8. Center CDC. Traumatic Brain Injury. *Traumatic Brain Injury* [Website]. Available at: http://www.cdc.gov/ncipc/tbi/TBI.htm. 2007.

9. Adams JH, Doyle D, Graham DI, et al. Diffuse axonal injury in head injuries caused by a fall. *Lancet.* 1984/// 1984;2:1420-1422.

10. Gennarelli TA. Mechanisms of brain injury. *JEmergMed.* 1993/// 1993;11(supp 1).5-11.

11. Grady MS, McLaughlin MR, Christman CW, et al. The use of antibodies targeted against the neurofilament subunits for the detection of diffuse axonal injury in humans. 1993/// 1993;52(2):143-152.

12. Smith DaM, DF. Axonal Damage in Traumatic Brain Injury. *The Neuroscientist.* 2000;6(6):483-495.

13. Thibault LE, Gennarelli TA, Margulies SS, et al. The Strain Dependent Pathophysiological Consequences of Inertial Loading on Central Nervous System Tissue. *Proceedings of the International Conference on the Biomechanics of Impact.* Lyon, France; 1990:191-202.

14. Morrison B, 3rd, Meaney DF, McIntosh TK. Mechanical characterization of an in vitro device designed to quantitatively injure living brain tissue. *Ann Biomed Eng.* 1998;26(3):381-390.

15. Ellis EF, McKinney JS, Willoughby KA, et al. A new model for rapid stretch-induced injury of cells in culture: characterization of the model using astrocytes. *J Neurotrauma.* 1995;12(3):325-339.

16. Pfister BJ, Weihs TP, Betenbaugh M, et al. An in vitro uniaxial stretch model for axonal injury. *Ann Biomed Eng.* 2003;31(5):589-598.